245

A STUDY OF MONOPULSE TRACKING RADAR SYSTEMS

by

SULTAN M. ZIA

B.E., B.M.S. College of Engineering
University of Mysore, India, 1962

866

A MASTER'S REPORT

submitted in partial fulfillment of the

requirements for the degree

MASTER OF SCIENCE

Department of Electrical Engineering

1965

Approved by:

[signature]
Major Professor

TABLE OF CONTENTS

INTRODUCTION

The tracking radars are classified in three major categories according to the techniques employed to obtain information about the position of a target with respect to the radar beam. These techniques are conical scan, sequentially lobed and monopulse.

The monopulse technique was developed for precision target tracking. Beam switching and conical scanning methods are not accurate due to the target scintillation. For example one of the principle difficulties in conical scan systems is the interaction between the lobing rate and the noise modulation components at the same frequency in the return signal. Noise modulation caused by the propeller rotation is particularly undesirable, since errors introduced by such high amplitude noise make it difficult to track a target (Dunn and Howard, 1958).

A technique for determining direction by comparing the returns from two or more antenna lobes simultaneously was developed to eliminate the source of errors present in conical scan and sequential lobing techniques. Furthermore, simultaneous lobing or often called monopulse method has the advantage of a higher data rate since three dimensional information about the target location is available from every received pulse in principle at least (Rhodes, 1959).

A review of some of the methods used prior to the development of monopulse is given below. In sequential lobing

techniques the magnitude of the angular error in one coordinate is obtained by alternately switching the antenna beam between two points (Figure 1-a). The difference in amplitude between the voltages thus obtained is a measure of angular displacement of the target from the switching axis, whereas its sign determines the direction of the error. The other technique known as the conical scanning, is a simple extension of the sequential lobing. In this technique an offset antenna beam is rotated continuously as opposed to the discontinuous stepping of the sequential lobing (Figure 1-b). The angle between the axis of rotation and the axis of the antenna beam is called the squint angle. The echo signal is modulated at the rotation frequency of the beam. The conical scan modulation is extracted from the echo signal and applied to a servo controlled system which continuously positions the antenna on the target. When the antenna is on the target, the line of sight to the target and the rotation axis coincide and the resulting conical scan modulation is zero.

However, because of the errors involved in the above two systems sequential lobing was further developed (Page, 1955) wherein a method was found to locate a target completely from the return of a single pulse. This possibility led to the term "monopulse" which was suggested originally by Budenbom at the Bell Telephone laboratories in 1946.

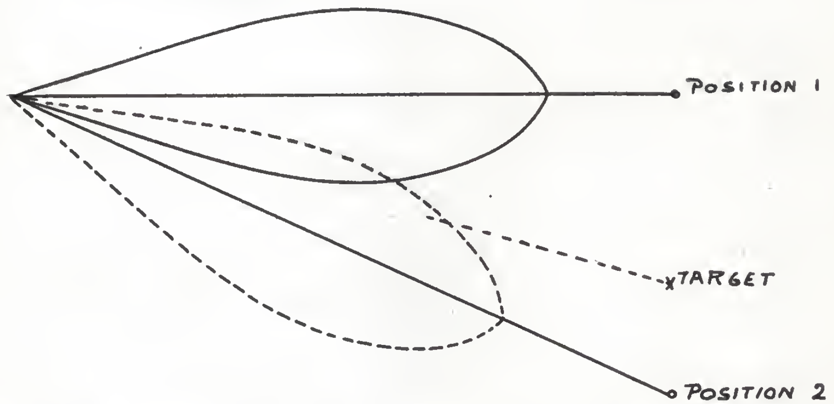


Figure 1-a. Polar representation of switched antenna pattern.

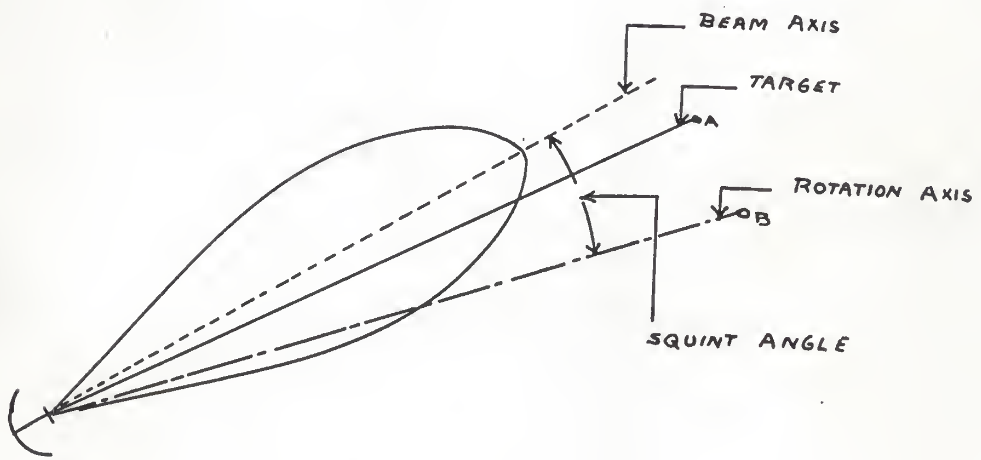


Figure 1-b. Representation of conical-scan tracking.

UNIFIED MONOPULSE THEORY

A number of techniques may properly be called monopulse. The various forms may appear to be independent and unrelated. The obstacle to a complete understanding of the concept was due to a lack of a definition, and a theory to explain the apparent differences between them. Such a definition is given here in the form of three postulates. It evolved as a part of the unified theory of the monopulse developed during the winter of 1956-57.

Three postulates of monopulse: The source of target angle information lies in the radiation patterns of the monopulse antenna. The form in which it appears depends on the way in which the return signals are compared and processed which in turn will determine the various types of monopulse that are possible. The essential characteristics of the various forms of monopulse may be deduced and developed into a unified theory from a set of three basic postulates. These are explicit statements of the physical characteristics common to all monopulse systems (Rhodes, 1955). The three postulates are as follows.

Postulate 1. The monopulse angle information appears in the form of a ratio.

The angle information is obtained by comparing pairs of received signals. The requirement that the comparison be in the form of a ratio implies that the angle output of a monopulse system will be a function only of the angle of

arrival, and thus independent of the absolute amplitudes of the return signal.

Postulate 2. The sensing ratio for a positive angle of arrival is the inverse of the ratio for an equal negative angle.

This postulate and the next imposed conditions of symmetry about the boresight on the angle-output function. The term inverse is defined in the group sense, i.e., any element times its inverse is the identity element.

If the multiplicative and additive sensing ratios are $\gamma m(u)$ and $\gamma a(u)$ respectively where u is itself a function of angle of arrival θ then Postulate 2 states that

$$\gamma m(u) = \frac{1}{\gamma m(-u)} \tag{1}$$

and $$\gamma a(u) = -\gamma a(-u) \tag{2}$$

The multiplicative inverse of a group element is its reciprocal; its identity element is unity. The additive inverse of a group element is its negative, its identity element being zero. The physical interpretation of the identity element is that it represents the value of the sensing ratio in the boresight direction.

Postulate 3. The angle-output function is an odd real function of the angle of arrival.

The angle output of a monopulse system must indicate magnitude and sense of the angle of arrival. This postulate hypothesizes that the angle output is a real function of the angle of arrival and that it has odd symmetry about the

boresight direction.

The angle output is a function of the sensing ratio $\gamma(u)$. With the exception of certain special cases $\gamma(u)$ is always complex being derived from antenna radiation patterns which are generally complex functions of angle. Thus the angle output will, in general, be expressed as a real function of the complex variable $\gamma(u)$. If one defines the angle output to be the real part of a complex angle detection function F( ) then Postulate 3 states that

$$\mathrm{Re}\, F\left[\gamma(u)\right] = -\mathrm{Re}\, F\left[\gamma(-u)\right] \qquad (3)$$

<u>The General Theory</u>. The operation of a monopulse system as defined by the three postulates may be described analytically by a sequence of mapping transformations of a function of a complex variable from one complex plane to another as shown below:

$U(\theta)$ →	$\gamma(u)$ →	$\gamma c(\gamma)$ →	$F(\gamma c)$ →	Re F
Angle of arrival	Angle sensing	Ratio conversion	Angle detection	Angle output

The first of these transformations transforms U, a fixed real function of angle of arrival θ, into the sensing ratio $\gamma(u)$ of Postulate 2. This in turn may be converted by an appropriate transformation into any one of the other forms of the sensing ratio admitted by the three postulates. Finally it is transformed into the angle detection function $F(\gamma)$ of Postulate 3, the real part of which represents the angle output of the system. In the following few paragraphs each of the

transformations is described in detail.

<u>Angle Sensing</u>. The first transformation in the sequence characterizing the monopulse system is the formation of the complex angle-sensing ratio. From the first and second postulates the sensing ratio will appear in one of the following forms.

$$\gamma m(u) = \frac{P(u)}{P(-u)} \tag{4}$$

$$\text{or } \gamma a(u) = \frac{Po(u)}{Pe(u)} \tag{5}$$

where P(u) is an arbitrary function of u, and Po(u) and Pe(u) are arbitrary odd and even functions of u respectively. A simple expression for $\gamma m(u)$ is obtained if P(u) and P(-u) are taken to be the complex antenna patterns. The function Po(u) and Pe(u) can then be taken to be the odd and even components of P(u) as

$$Po(u) = \tfrac{1}{2}\left[P(u) - P(-u)\right] \tag{6}$$

$$Pe(u) = \tfrac{1}{2}\left[P(u) + P(-u)\right] \tag{7}$$

The ratios $\gamma m(u)$ and $\gamma a(u)$ are thus arbitrarily defined and are not independent. Either one of these can be expressed in terms of the other by a bilinear transformation such as

$$\gamma a(u) = \frac{\gamma m(u) - 1}{\gamma m(u) + 1} \tag{8}$$

In general the pattern of an antenna is a complex function of

angle and may be represented by

$$P(u) \overset{\Delta}{=} p(u)\ e^{j\phi(u)} \tag{9}$$

where p(u) and $\phi(u)$ are the far-field amplitude and phase patterns respectively.

Ratio Conversion. Once the angle-sensing ratio has been formed, it can be converted into any other ratio satisfying the monopulse postulates by a transformation labelled as the second in the sequence describing the operation of a monopulse system. The most general analytic transformation with a one-to-one correspondence between all points in two simple complex planes is a bilinear transformation of the form

$$w = \frac{az + b}{cz + d} \tag{10}$$

where $z = x + iy$
$w = u + iv$

It has the property of mapping 'circles' into 'circles'. One particular example of ratio conversion has already been shown in relating $\gamma m(u)$ to $\gamma a(u)$ in Equation 5. Ratio conversion offers a means of controlling the form of angle information from the angle sensor to the angle detector.

Angle Detection. The third and final transformation in the monopulse transformation sequence is the formation of the angle detection function $F(\gamma)$. The angle detection function may be any arbitrary function whose real part is odd and has continuous first and second derivatives.

Current monopulse practice is limited entirely to simple sensing of the angle of arrival, i.e., to either pure amplitude or pure phase sensing. Therefore theory associated with these may be deduced from the general theory.

Consider first the case of pure amplitude sensing. The angle information extracted by the monopulse antenna from the returned wave is contained strictly in the amplitude patterns p(u) and p(-u) of the antenna. The effective phase patterns $\phi(u)$ and $\phi(-u)$ must be made identical. If the complex patterns have phase centers, as is frequently the case in practice, any separation will introduce a corresponding change in the angle measurement.

With identical phase patterns the two sensing ratios involve only pattern amplitudes.

$$\gamma m(u) = \frac{p(u)}{p(-u)} \tag{11}$$

$$\text{and } \gamma a(u) = \frac{p(u) - p(-u)}{p(u) + p(-u)} \tag{12}$$

Angle information is contained solely with amplitude ratio $\rho(u)$ defined by

$$\rho(u) \triangleq \frac{p(u)}{p(-u)}$$

$$\text{and hence } \gamma m(u) = \rho(u) \tag{13}$$

$$\text{and } \gamma a(u) = \frac{\rho(u) - 1}{\rho(u) + 1} \tag{14}$$

Consider next the case of pure phase sensing. The angle

information is contained strictly in the phase patterns $\phi(u)$ and $\phi(-u)$. Here the effective amplitude patterns must be made identical. Hence the two sensing ratios are

$$\gamma m(u) = \frac{e^{j\phi(u)}}{e^{j\phi(-u)}} \tag{15}$$

$$\text{and } \gamma a(u) = \frac{e^{j\phi(u)} - e^{j\phi(-u)}}{e^{j\phi(u)} + e^{j\phi(-u)}} \tag{16}$$

Angle information is then contained solely in the phase difference $\theta(u)$ defined by

$$\theta(u) \triangleq \phi(u) - \phi(-u) \tag{17}$$

Therefore

$$\gamma m(u) = e^{j\theta(u)} \tag{18}$$

$$\text{and } \gamma a(u) = j \tan \frac{\theta(u)}{2} \tag{19}$$

The Equations (15), (16), (17), (18), (19) constitute the various forms of pure amplitude or pure phase sensing permitted by the monopulse postulates. Hence any type of the sensor can be characterized by one of the above sensing functions.

The additive sensing functions, although not independent of the multiplicative sensing functions, nevertheless are significant to the special theory as these are both amplitude functions on the real and the imaginary axes respectively as shown in Figure 2. Except for the 90° phase difference between the two it would be impossible to tell whether amplitude or

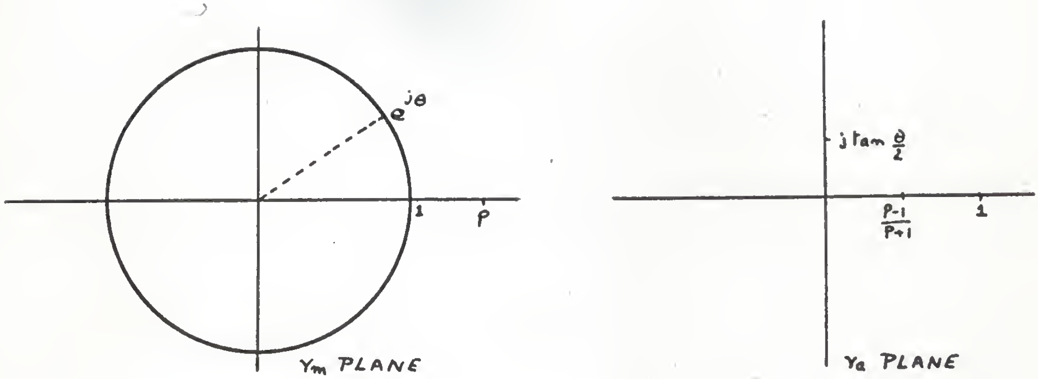


Figure 2. The four Υ - plane contours admitted by the monopulse theory.

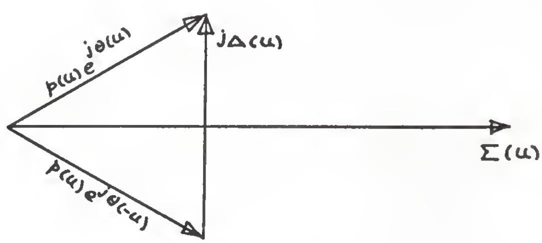


Figure 3. Relationship between the complex-pattern functions and their sum and difference for pure phase sensing.

phase sensing had been used to obtain any given function. In this sense therefore the additive sensing functions are equivalent and hence the sensing functions $\rho(u)$ and $\theta(u)$ are equivalent themselves, i.e., the amplitude function $\rho(u)$ is equivalent to the phase function $\theta(u)$ and conversely, where the two are related by the equivalence equation (Rhodes, 1959)

$$\operatorname{Tan} \frac{\theta(u)}{2} = \frac{\rho(u) - 1}{\rho(u) + 1} \tag{20}$$

This equivalence between amplitude and phase sensing is significant in that any kind of sensor can be described in terms of either sensing functions or in terms of the sum-and-difference of the sensing function $\frac{\Delta(u)}{\Sigma(u)}$

$$\text{Where } \frac{\Delta(u)}{\Sigma(u)} \triangleq \frac{\rho(u) - 1}{\rho(u) + 1} \quad \text{for amplitude sensing}$$
$$= \operatorname{Tan} \frac{\theta(u)}{2} \quad \text{for phase sensing} \tag{21}$$

The symbols $\Delta(u)$ and $\Sigma(u)$ designate the magnitudes of the difference and sum respectively of the pattern functions. In case of pure amplitude sensing

$$\Delta(u) = p(u) - p(-u)$$
$$\text{and } \Sigma(u) = p(u) + p(-u) \tag{22}$$

because pattern functions are in phase. In case of pure phase sensing the patterns have equal amplitudes, hence their difference and sum are in phase quadrature. Referring to

Figure 3

$$\Delta(u) = 2p(u) \, \mathrm{Sin} \, \frac{\theta(u)}{2}$$

$$\text{and} \sum(u) = 2p(u) \, \mathrm{Cos} \, \frac{\theta(u)}{2} \tag{23}$$

Thus the concept of monopulse has been defined by a set of three postulates. On the basis of this definition which is simply an explicit statement of the fact that the angle output is independent of the amplitude level of the received signals and that it has odd symmetry about the boresight, all known types of monopulse may be derived as special cases of a complete general theory. The theory of these cases does even more than provide a consistent explanation of the origin of the known types of monopulse and their interrelationships; it also shows that these form a mutually exclusive set, i.e., that these and no more are possible within the postulated structure of this theory.

The principle result of the general theory is that the operation of a monopulse system can be described analytically by a sequence of mapping transformations of a complex variable from one complex plane to another. Two transformations are common to all monopulse systems, namely, mapping of a fixed function of angle of arrival onto the angle sensing plane and mapping of the sensing ratio onto the angle detection plane. The first is controlled by the angle sensor, the second by the angle detector. A third transformation may be performed in

between these two basic transformations in order to convert the sensing ratio formed by the angle sensor into whatever form is desired for angle detection.

In the general theory the sensing-ratio and the angle-detection function may be arbitrary complex functions satisfying the monopulse postulates. The special theory is restricted specifically to those particular cases of the general case and involves either pure amplitude or pure phase sensing. Sensing in the special theory is always described by one of three functions, amplitude $\rho(u)$, phase $\theta(u)$, or sum-and-difference $\left[\Delta(u)/\sum(u)\right]$. The sum-and-difference sensing function is related to both the amplitude and phase sensing functions, a relationship which implies an equivalence between the latter two. Thus there are two independent, although equivalent, forms of special sensing. When limited to these particular forms there are three and only three distinct classes of angle detection possible and hence there are three distinct classes of special monopulse possible.

MONOPULSE SYSTEMS

In the last section a general theory was derived from three fundamental postulates defining the concept of monopulse, and the basic properties of a special theory were outlined. Some of the techniques by which the various forms of monopulse can be physically realized are described here. First a two dimensional operation is outlined and later the dual plane systems are described.

The basic components of a monopulse system are shown in Figure 4 in the sequence of functions performed. The angle of arrival is sensed by the monopulse antenna, which is the primary and sometimes the only element of the angle sensor. The angle information appears in the form of two functions whose ratio called the sensing ratio, is formed later. The two functions must either be mirror images of each other (for multiplicative sensing) or one must have odd and the other an even symmetry (for additive sensing) about the boresight axis. After sensing the angle of arrival the sensing ratio may be converted into any other form desired by performing a bilinear transformation and detected to obtain angle output function. The purpose of ratio conversion may either be to convert the angle information from amplitude into phase or vice versa. It is usually performed at the carrier frequency using passive components for reasons of simplicity and stability. When the system is used in a radar, duplexing can be introduced either in the angle sensor or in the ratio converter. All the rest of the system

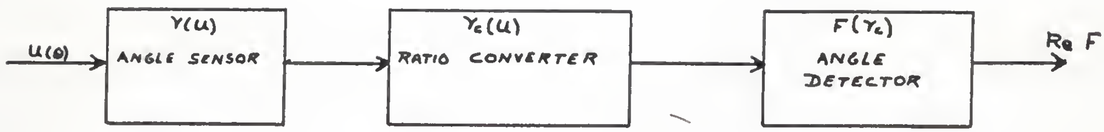


Figure 4. Functional block diagram of a monopulse system.

following the ratio converter may be lumped together under the term of angle detector. The angle detector usually contains all of the active components in the system, including the amplifiers and comparison circuitry that form the ratio and the angle detection function and that produce the real part of the angle detection function at the output. In the following few paragraphs each of the components of the system is described in detail.

Angle Sensors. The source of raw data on the angle of arrival of an incident wave is a pair of signals extracted from that wave by the sensing antenna. These are usually in the form of simple functions that differ only in magnitude or in phase. The general theory of monopulse allows these functions to be complex but this area has not been explored as yet. The two types of antennas commonly in use for simple sensing are the reflector and the lens illuminated by directional point sources.

A parabolic reflector excited symmetrically by a primary source at the focal point will produce a symmetrical pattern with a spherical phase front. Two such reflectors constitute an interferometer with phase centers spaced a distance S apart. Their amplitude patterns will be identical but their phase patterns will differ by an amount equal to (Page, 1955)

$$\theta(u) = \frac{2\pi}{\lambda} S \sin \phi \tag{24}$$

as shown by Figure 5. Where $\theta(u)$ is the phase difference due to the difference in lengths R_1 and R_2.

The interferometer can be used for pure phase sensing.

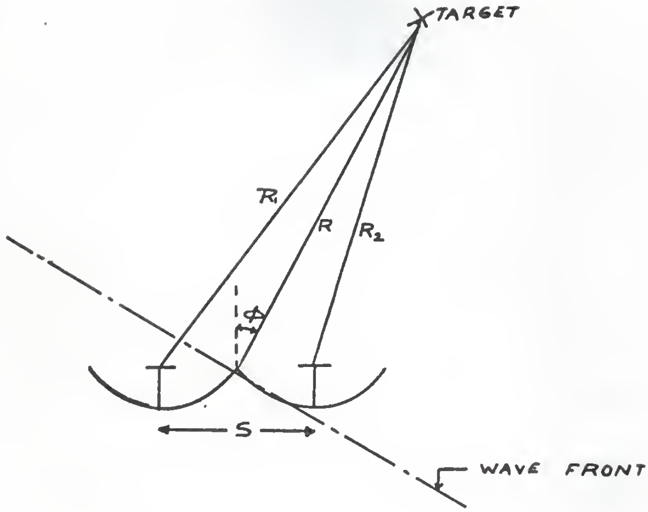


Figure 5. Wavefront phase relationships in phase-comparison-monopulse radar.

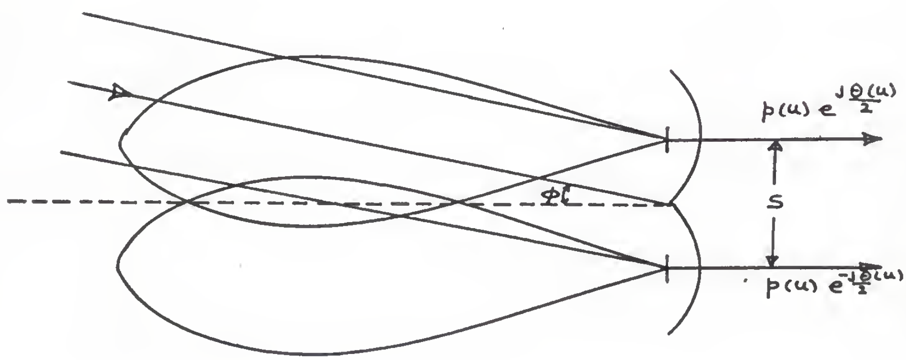


Figure 6. Monopulse reflector type antennas for phase sensing of the multiplicative sensing function.

The signals received can be used directly for multiplicative phase sensing or for additive phase sensing by forming their sum and difference in a hybrid as shown in Figures 6 and 7 respectively.

If the primary source illuminating a parabolic reflector is displaced laterally from the focal point F by a small distance Δx, the phase center will remain close to its original position but the amplitude pattern will be squinted off the boresight axis at an angle approximately $\Delta x/f$. A pair of feeds displaced symmetrically from the focal point will then produce symmetrically overlapping amplitude patterns whose ratio indicates angle of arrival. The two received signals can be used directly for multiplicative sensing as shown by Figure 8, or by forming their sum and difference for additive amplitude sensing as shown by Figure 9. For each reflector type of antenna there corresponds an analogous lens type antenna.

Ratio Converters. Any of the four special sensing ratios may be converted into any of the others by the use of ratio converters. For example a short slot complex converts an amplitude sensing function into its equivalent phase sensing function and vice versa, without changing its realizable angular range or boresight sensitivity (Riblet, 1952). In its broadest sense the purpose of ratio conversion may be more than transformation of one sensing function into another. It may also be used to alter the realizable angular range and boresight sensitivity and to provide a means for duplexing.

Angle Detectors. Only three classes of angle detection

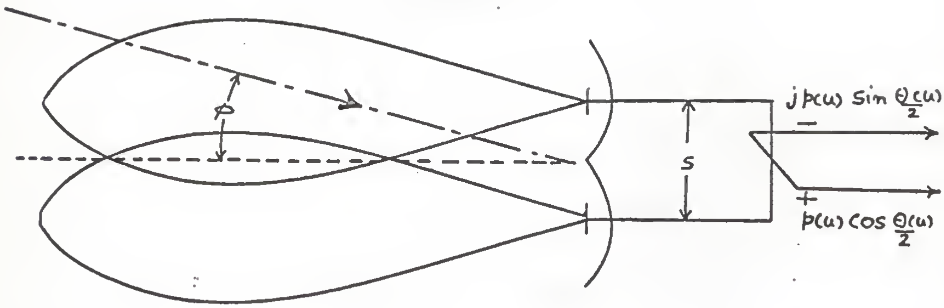


Figure 7. Monopulse reflector type antenna for phase sensing of the additive sensing function.

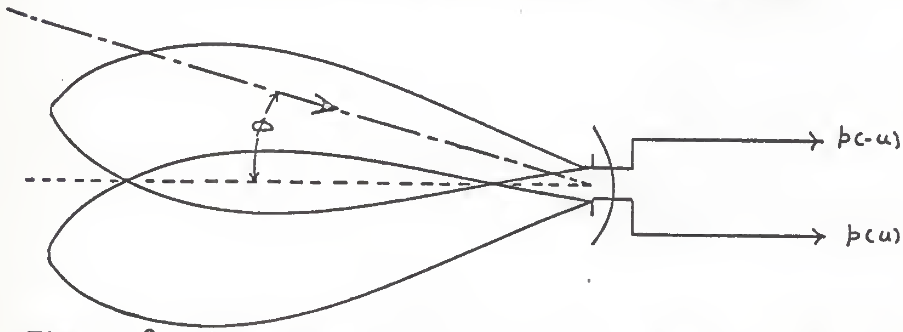


Figure 8. Monopulse reflector type antenna for amplitude sensing of the multiplicative sensing function.

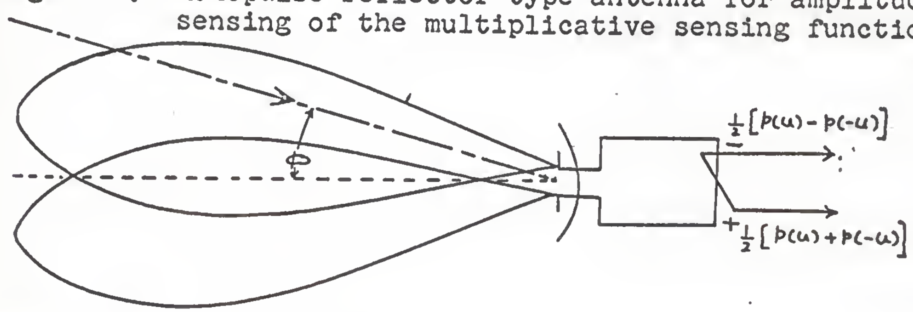


Figure 9. Monopulse reflector type antenna for amplitude sensing of the additive sensing function.

are admitted by the special theory. The three classes are sum and difference, pure amplitude and, pure phase. There is an unlimited number of specific forms of angle detection possible for each class, however, the only restriction being that the angle output function (real part of the angle detection) be odd and that it and its first and second derivatives be continuous.

The circuit for sum and difference pattern angle detection is illustrated in Figure 10. The two r.f. signals from the ratio converter are heterodyned with a local oscillator to produce an intermediate frequency suitable for amplification. By employing a common local oscillator for the two channels, symmetry of the two signals is preserved and coherence between channels is maintained. After mixing, these two signals are amplified and compared. The angle detection function for this class of angle detectors is simply the sensing ratio itself in the case of amplitude sensing, and sensing ratio rotated 90^o in the case of phase sensing. The angle output of the system is just the angle detection function $(\Delta(u)/\sum(u))$. The ratio is formed by the normalization property of the amplifiers. The normalization is introduced in the form of instantaneous automatic gain control (IAGC). An IAGC voltage is developed in the sum channel and used to control the gain of both channels. The result in effect, is to normalize both the sum-and-difference signal amplitudes with respect to the amplitude of the sum signal. The output of the sum channel then remains constant in time, ideally, and the output of the difference channel becomes

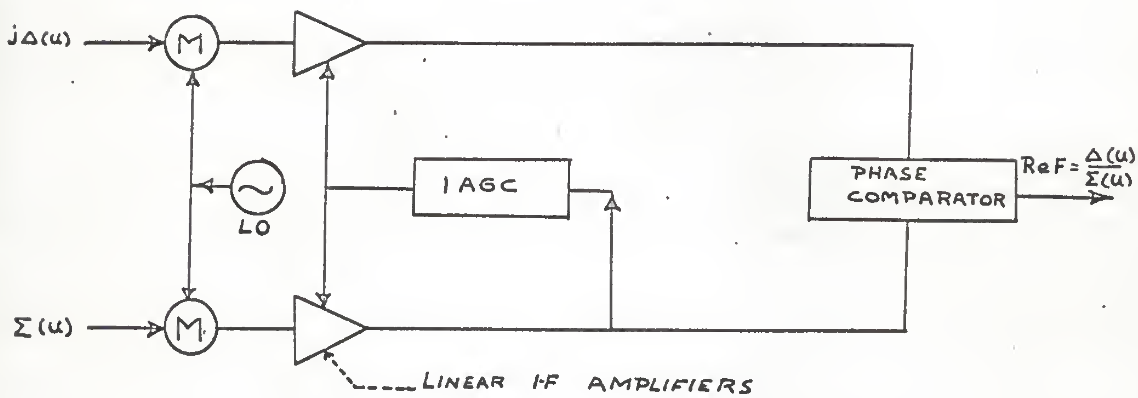


Figure 10. Angle detection circuit.

the ratio $\left[\Delta(u) / \sum(u)\right]$. For the angle detector mentioned above the comparator may be either the conventional phase comparator or the extended range phase comparator (Kirkpatrick, 1956) as shown in Figure 11, where

$$\text{Re } F = \left|\gamma + e^{-j\beta l}\right| - \left|e^{-j\beta l} + 1\right| \qquad (25)$$

The range of angle scanning with the conventional phase comparator is limited to that corresponding to a range of phase of 180°, but the maximum unambiguous range of the angle sensor itself is frequently greater than this. The Kirkpatrick comparator extends this angular range. The detection portion of this circuit is the same as in the conventional phase comparator consisting of linear rectifiers and a differencing network. The essential difference lies in the way the signals are combined before detection. In both cases the angle output is the difference between magnitudes of the complex voltages appearing at the detector diodes.

$$\text{Re } F = \left|V_1\right| - \left|V_2\right| \qquad (26)$$

Consider the circuit of Figure 12 which is a part of the above circuit illustrating the division of voltages. Current i generated by γ, divides at the junction of the two parallel impedances, one of which is a transmission line terminated in its characteristic impedance R_o and the other is R_o itself. Since the input impedance of a transmission line terminated in its characteristic impedance is just its characteristic

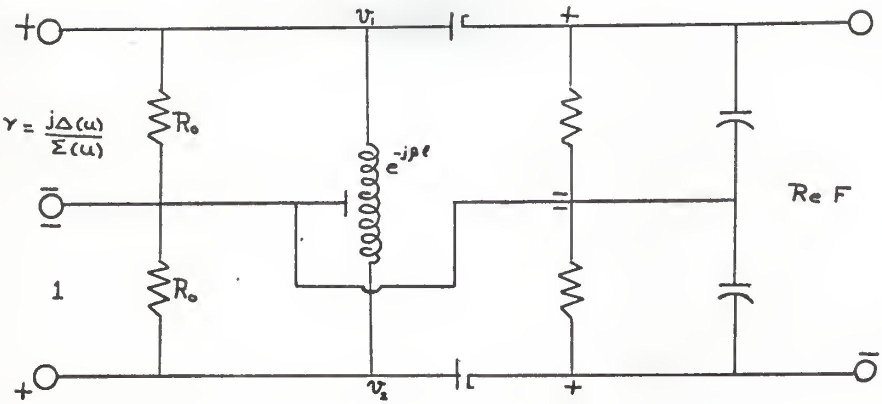


Figure 11. Extended-range phase comparator, (Kirkpatrick, 1956).

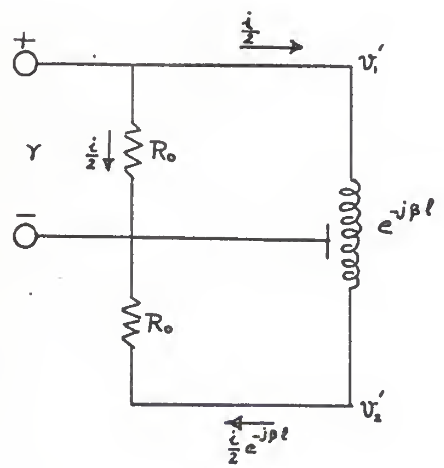


Figure 12. A portion of the Kirkpatrick comparator driven by the source γ.

impedance the current i divides equally into the two circuits. The two components generated by γ are

$$V_1^{\ 1} = \gamma$$

$$V_2^{\ 1} = \gamma e^{-j\beta l}$$

Similarly for the input voltage of unity applied to the bottom resister R_o of Figure 12, the components $V_1^{\ 1}$ and $V_2^{\ 1}$ generated are

$$V_1^{\ 1} = e^{-j\beta l}$$

and $V_2^{\ 1} = 1$

Hence by super position

$$\text{Re } F = \left| \gamma + e^{-j\beta l} \right| - \left| \gamma e^{-j\beta l} + 1 \right| \qquad (27)$$

$$\text{But } \gamma = j \left[\frac{\Delta(u)}{\sum(u)} \right] \qquad (28)$$

Hence

$$\text{Re } F = \left| j\frac{\Delta u}{\sum(u)} + e^{-j\beta l} \right| - \left| j\frac{\Delta(u)}{\sum(u)} e^{-j\beta l} + 1 \right| \qquad (29)$$

When $\beta l = \pi/2$, the above case reduces to conventional phase detector. But for $\beta l < \pi/2$ the angular range is extended to a value approaching the maximum of 360^o as βl approaches zero. This is indicated in Figure 13. The unambiguous angular range is limited by the conventional phase comparator to a range of $-90^o < \theta < 90^o$. So is the Kirkpatrick for $\beta l = \pi/2$. However

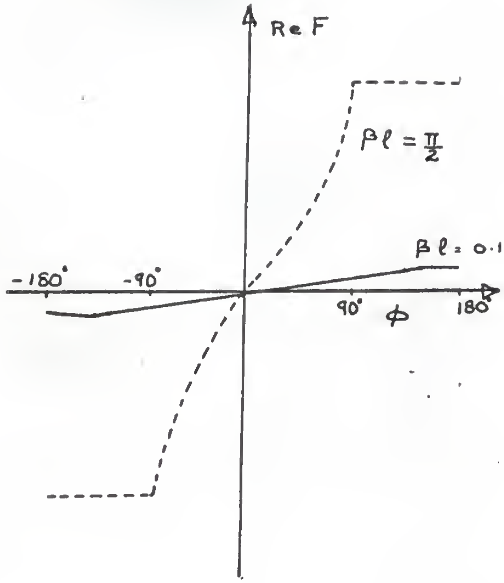


Figure 13. Angle output function from the Kirkpatrick comparator.

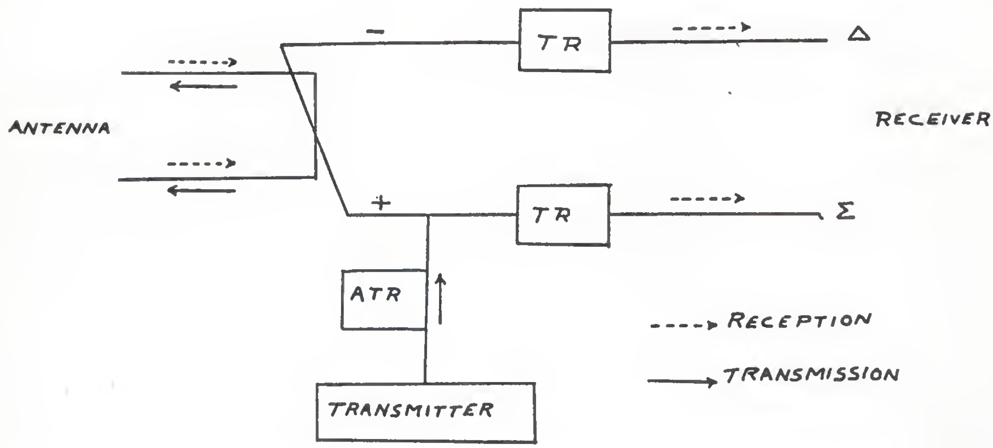


Figure 14. A sum-and-difference monopulse radar duplexer.

for $\beta l < \pi/2$ the angular range is extended beyond that of conventional comparator to the full 360°.

Duplexing. Since the concept of monopulse is limited strictly to reception, little mention has been made as yet of the problems of introducing a transmitter into the system when it is to be used as part of a radar. Generally speaking the transmitter portion of a monopulse radar is much the same as in any conventional pulse radar. Two important differences do exist, however, in the problems associated with duplexing. Monopulse duplexing is complicated by the necessity for multiple antenna feeds and receiving channels, in contrast to usual single-feed and receiving channel of conventional radar. Duplexing problems may be avoided altogether by using separate transmitting and receiving antennas, but in many cases this is far from the optimum use of the antenna aperture available. Therefore duplexing is a necessity if the same antenna is to be used for both transmission and reception.

Two general problems are associated with monopulse duplexing. One is that of exciting multiple feeds by a common source in such a way that the source is effectively disconnected from them during the interpulse period. The other is protection of the receivers from the peak pulse power during transmission. If the sum and difference of the signals received are formed directly at the antenna, both of the duplexing problems can be solved by the use of conventional duplexing techniques. The transmitter can be connected to the same line to excite the two feeds equally, thereby producing a transmitted pattern

with symmetry in both principle planes. On transmission the pulse power opens the anti-transmit-receive (ATR) switch and shorts the TR switches to feed the full power into the sum arm which then splits equally at the two antenna feeds. On reception the ATR switch disconnects the transmitter from the sum line while the TR switches open to pass the sum and difference of the received signals unimpeded to the angle detector, either directly or through a suitable ratio-conversion network.

A figure showing the connections of the duplexer to the monopulse system is as shown in Figure 14. A complete system diagram of the amplitude comparison-monopulse tracking radar for a single angular coordinate is shown in Figure 15. The output of the phase sensitive detector and the sum channel (range information) are shown displayed on the A-scope. The sum channel signal operates the A-scope just as in a normal radar. It gives an indication of target range by deflecting a beam upward, generating a pip. The output of the phase sensitive detector, however, modifies the scope sweep to deflect the target pip either to the right or to the left depending upon the sign of the angular error. The amount of leaning is a measure of the magnitude of the angular error.

The output of this system may also be used to perform automatic tracking. The angular error signal may actuate a servo controlled system to position the antenna, and the range output from the sum channel may be fed into an automatic range tracking unit.

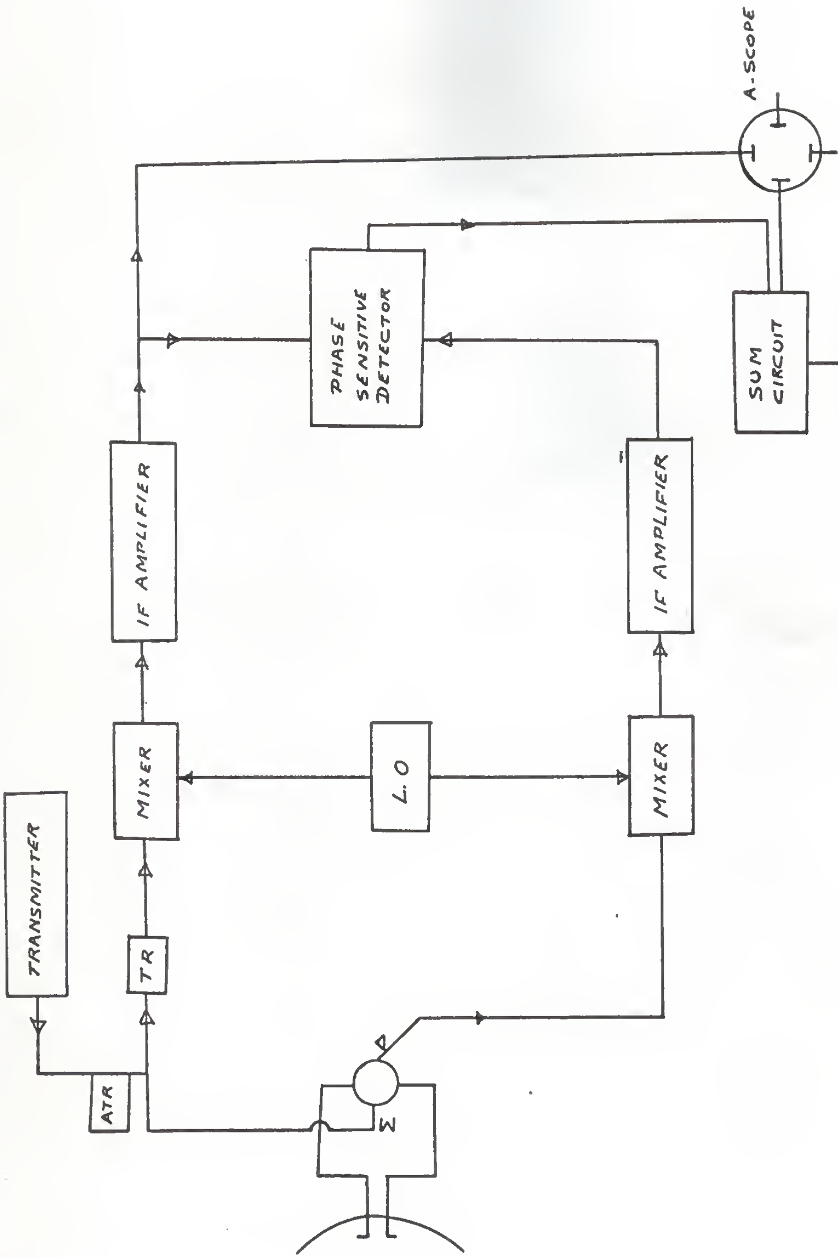


Figure 15. Block diagram of amplitude-comparison-monopulse radar in one angular coordinate (Skolnik, 1962).

The direction of the angular error is determined by comparing the phase of the difference signal with the phase of the sum signal. If the sum signal in the IF portion of the receiver were $A_s \cos w_{if}t$, the difference signal would be either $A_d \cos w_{if}t$ or $-A_d \cos w_{if}t$ ($A_s > 0$, $A_d > 0$) depending on which side of center the target is. Since $-A_d \cos w_{if}t = A_d \cos w_{if}(t + \pi)$, the sign of the difference signal may be measured by determining whether the difference signal is in phase with the sum signal or 180^o out of phase.

In the following paragraph the error signal of the amplitude comparison monopulse radar is derived (Skolnik, 1962). If an antenna pattern is Gaussian, the one way (voltage) pattern from one monopulse beam is

$$G(\theta) = G_o^{\frac{1}{2}} \exp\left(-a^2\theta^2/_2\right) \qquad (30)$$

where G_o is the maximum antenna gain.

θ = angle between antenna beam axis and target axis

a^2 = constant = $2.776\ \theta^2{}_B$

where θ_B is antenna beam width measured between 3 - db or half-power points of antenna patterns.

Referring to the diagram of Figure 16

$$(R\theta)^2 = (R\theta_q)^2 + (R\theta_t)^2 - 2\ R^2\theta_q\theta_t \cos(\phi - \phi o) \qquad (31)$$

Assuming $(\phi - \phi o)$ to be very small, the equation (31) becomes

$$\theta^2 = \theta_q{}^2 + \theta_t{}^2 - 2\ \theta_q\theta_t \qquad (32)$$

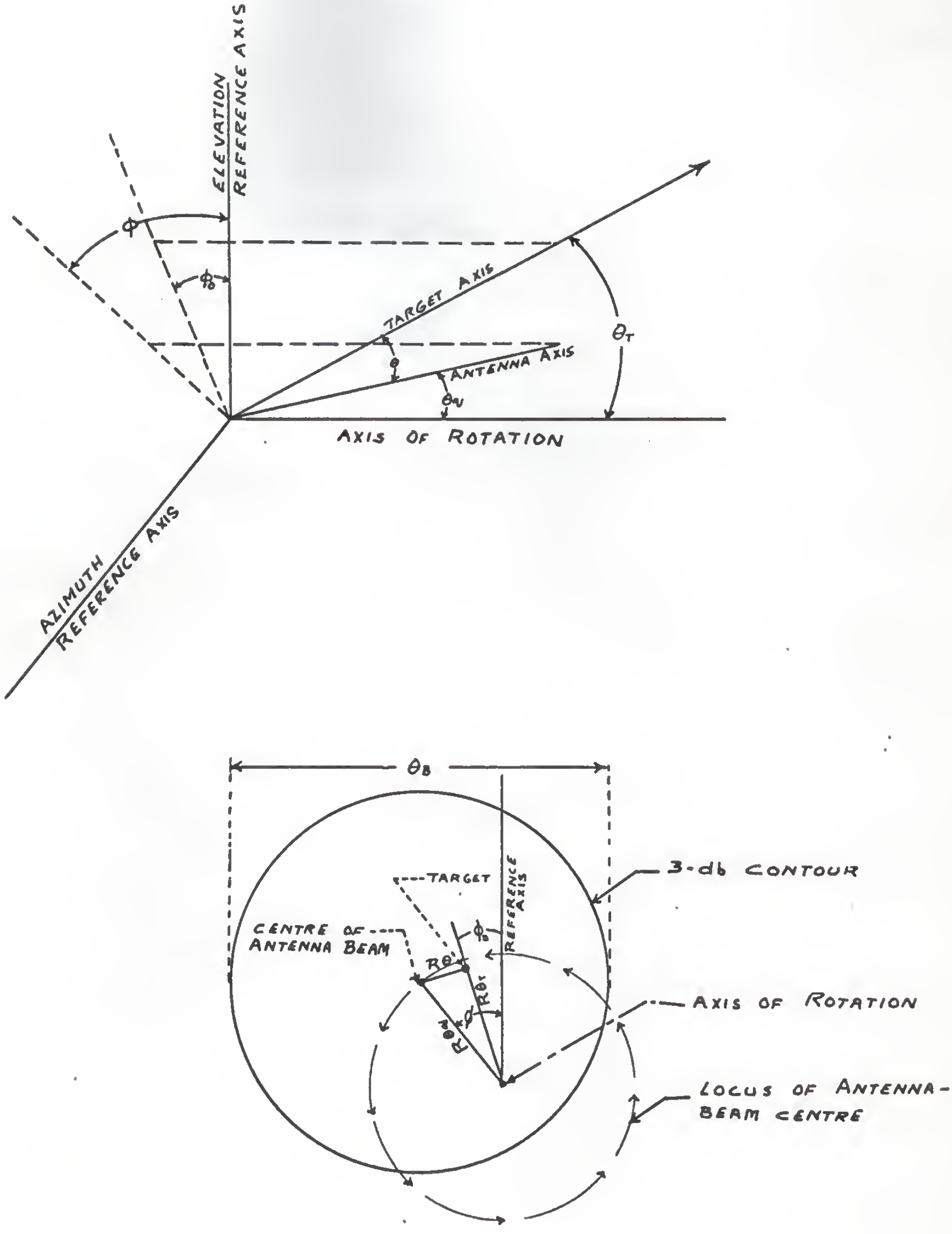


Figure 16. Geometry and symbols for derivation of monopulse error signal (Skolnik, 1962).

Therefore

$$\theta^2/2 = \tfrac{1}{2}(\theta^2_q + \theta^2_t) - \theta_q\theta_t \qquad (33)$$

Hence

$$G(\theta) = G_o^{\frac{1}{2}} \exp\left[-\frac{a^2}{2}(\theta^2_q + \theta^2_t)\right] \exp\left[a^2\theta_q\theta_t\right] \qquad (34)$$

This is the antenna pattern of one beam. By symmetry, the antenna pattern of the other beam would be

$$G(\theta) = G_o^{\frac{1}{2}} \exp\left[-\frac{a^2}{2}(\theta^2_q + \theta^2_t)\right] \exp(-a^2\theta_q\theta_t) \qquad (35)$$

One way voltage sum pattern is

$$2\ G_o^{\frac{1}{2}} \exp\left[-\frac{a^2}{2}(\theta^2_q + \theta^2_t)\right] \cos h\ a^2\theta_q\theta_t \qquad (36)$$

and the one way voltage difference pattern is

$$2\ G_o^{\frac{1}{2}} \exp\left[-\frac{a^2}{2}(\theta^2_q + \theta^2_t)\right] \sin h\ a^2\theta_q\theta_t \qquad (37)$$

Since the transmitted voltage is of the sum pattern, the two way IF difference signal voltage is

$$2\ K \exp\left[-a^2(\theta^2_q + \theta^2_t)\right] \sin h\ 2\ a^2\theta_q\theta_t \cos 2\ f_{if}t \qquad (38)$$

Where K is a constant determined by the parameters of the radar equation.

The two way antenna pattern of the sum channel is

$$4K \exp\left[-a^2\ (\theta^2_q + \theta^2_t)\right] \cos h^2a^2\theta_q\theta_t \qquad (39)$$

The sum and difference signals are multiplied in the phase sensitive detector to give the error signal. The output of the

phase sensitive detector is a d.c. voltage whose amplitude is proportional to the product of sum and difference amplitudes. Hence the error signal is

$$c_1 \exp \left[-2a^2(\theta^2{}_q + \theta^2{}_t)\right] \cos h^2a^2\theta_q\theta_t \sin h \; 2a^2\theta_q\theta_t \qquad (40)$$

For small angular errors this reduces to

$$c_2\theta_t \qquad (41)$$

Where c_1 and c_2 are constants. Thus the error signal in the monopulse radar is a linear function of the angular displacement of the target from the axis, assuming small angular displacements.

A complete system diagram of the phase comparison monopulse radar for a single angular coordinate is shown in Figure 17 (Blewett, Hansen, Troell and Kirkpatrick, 1944). In the system shown two antennas are shown side by side. These are directive antennas, one of which is connected to the transmitter and receiver as in the conventional radar, while the other antenna feeds a receiver only. The transmitter is shown connected to the antenna via a duplexer. In practice a second duplexer may be inserted in front of the other receiver, not so much for protection, but to balance the phase shifts in the two channels. The two receiving channels should be identical. The R.F. echo signals are heterodyned to an intermediate frequency with a common local oscillator. The outputs of the two IF amplifiers are compared in a phase detector the output of which is the error signal which serves as the input to the servo controlled

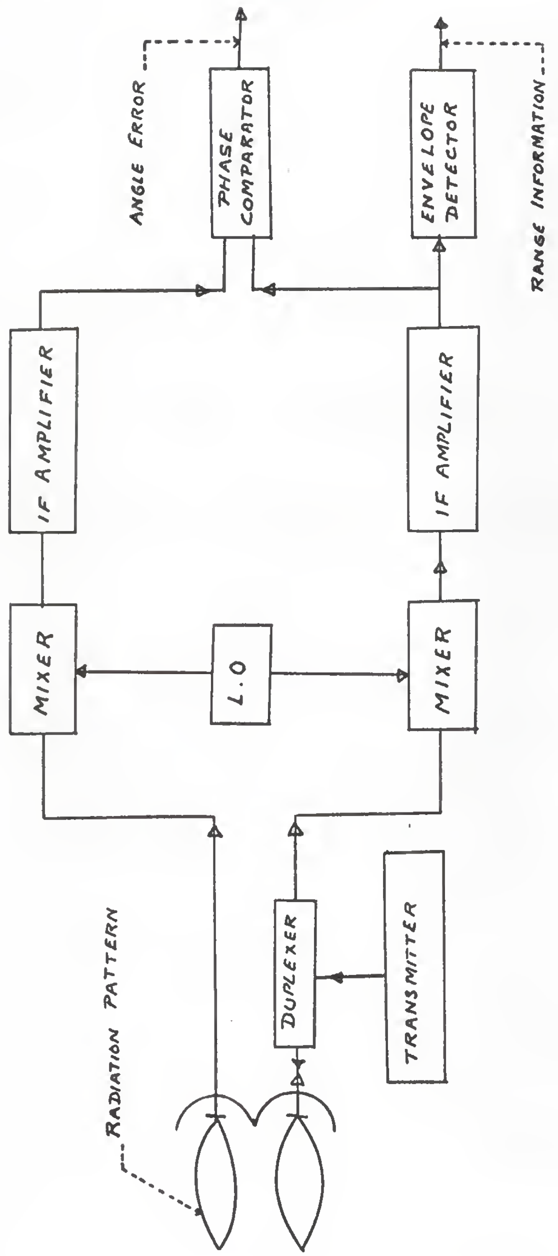


Figure 17. Block diagram of phase-comparison-monopulse radar in one angular coordinate, (Page, 1955).

loop to position the antenna.

Dual-plane monopulse systems: Amplitude comparison radar. The block diagram of the system is shown in Figure 18 (Skolnik, 1962). The cluster of four feeds generates four partially overlapping antenna beams. The feeds might be used with either a parabolic reflector or a lens. All four feeds generate the sum pattern. The difference pattern in one plane is formed by taking the sum of two adjacent feeds and subtracting this from the sum of the other two adjacent feeds. The difference pattern in the orthogonal plane is obtained by adding the differences of the orthogonal adjacent pairs. A total of four hybrid junctions generate the sum channel, the azimuth difference channel and the elevation difference channel. Three separate mixers and IF amplifiers are shown one for each channel. Two phase comparators extract the angle error information, one for azimuth and the other for elevation. Range information is extracted from the output of the sum channel after amplitude detection.

Two beam sensing (Rhodes, 1959). Dual plane angle sensing can be realized directly from a single pair of beams. The simplest form of dual plane angle sensor is obtained simply by squinting the two beams of a single plane interferometer as shown in Figure 19. The angle sensing function in the principal azimuth plane is phase, and in the principal elevation plane is amplitude. This constitutes a simple sensing in the two principal planes, consistent with the special theory, even though it is complex sensing in any other plane because of its unsymmetrical character. A source displaced off the boresight

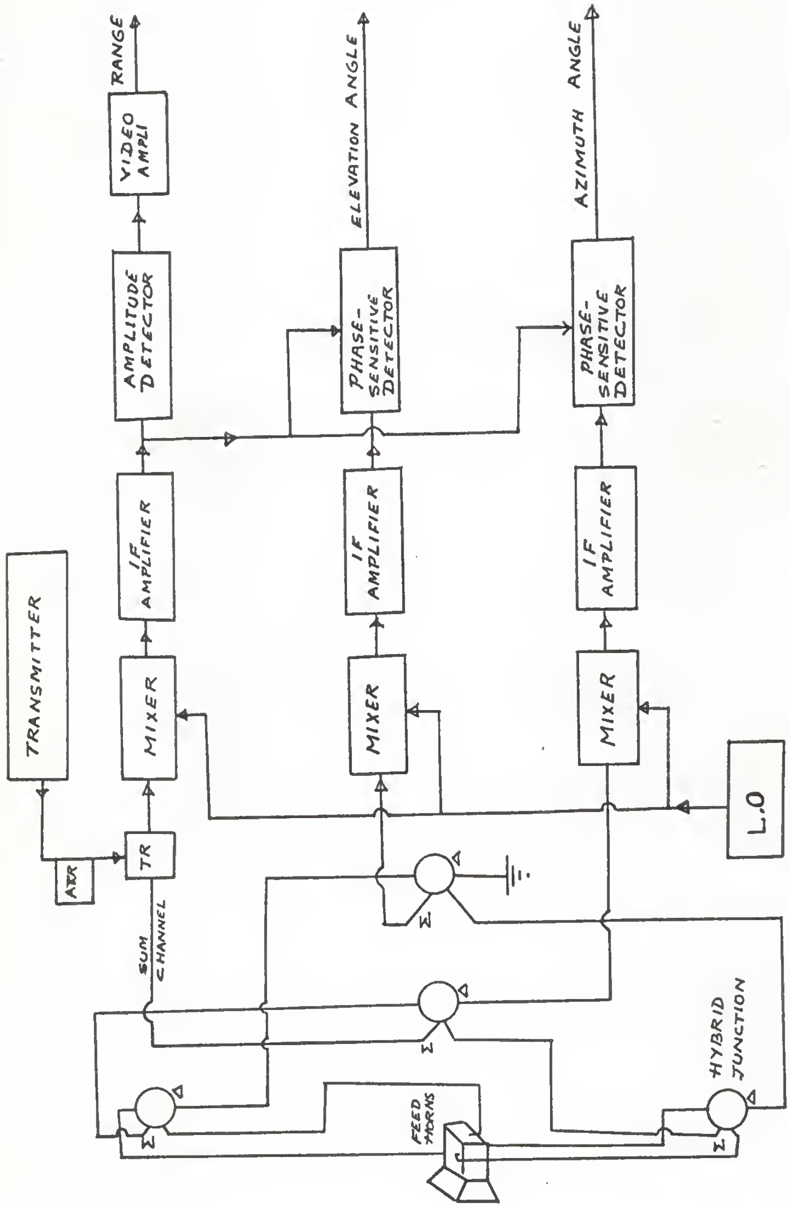


Figure 18. Block diagram of two-coordinate (azimuth and elevation) amplitude-comparison-monopulse tracking radar (Skolnik, 1962).

axis will induce voltages that differ in phase according to its azimuth displacement and that differ in amplitude according to its elevation displacement. On the boresight axis the two voltages are equal and in phase. The difference signal then passes through zero on the boresight. With the source in one of the two principle planes the angle sensor operates simply as an ordinary single-plane sensor. In the principle azimuth plane the signals received are of equal amplitude and the sensor reduces to the single-plane equivalent of an interferometer. In the principle elevation plane the signals received are in phase and the sensor reduces to the single-plane equivalent of a pair of squinted beams. For small displacements from either principle plane the components of the complex signal parallel and perpendicular to the sum signal approximate, respectively, the elevation and azimuth error signals. This approximation becomes poorer for sources farther from the boresight, however, because both azimuth and elevation become intermixed in each of the two components. This field of complex sensing is still open for research.

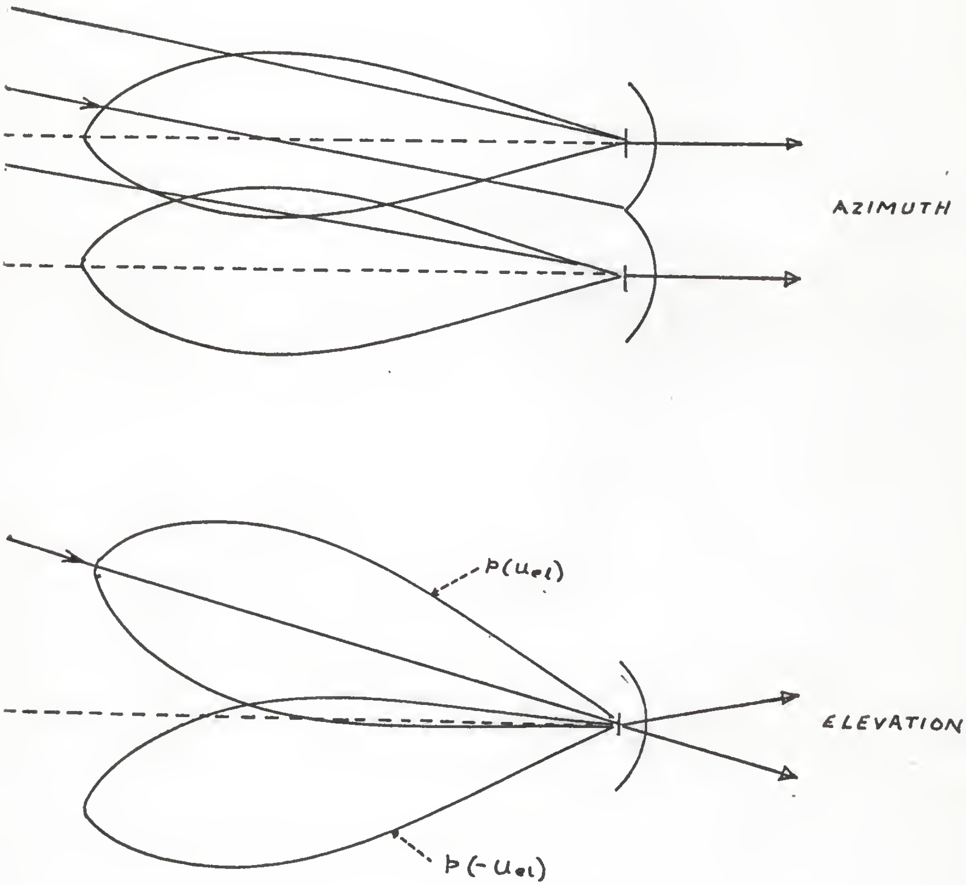


Figure 19. A two beam angle sensor. The azimuth angle-sensing function is phase, while the elevation angle-sensing function is amplitude.

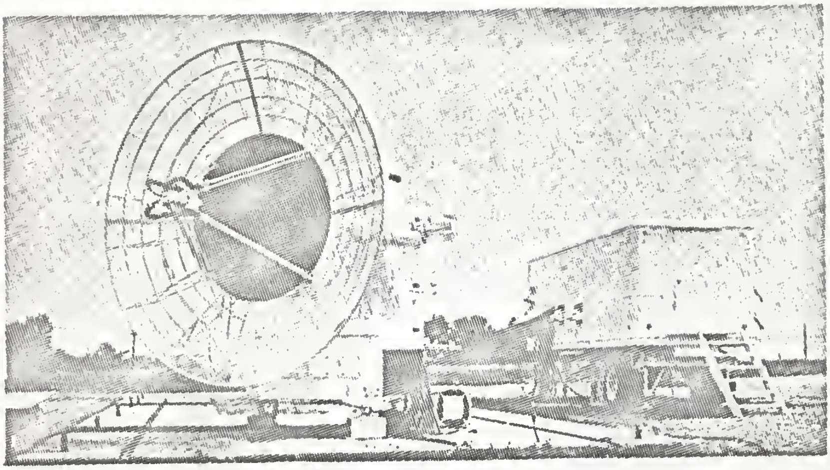


Figure 20. AN/FPS - 16 Monopulse tracking radar.

AN/FPS - 16 Instrumentation Radar Characteristics
(Barton and Sherman, 1960)

Antenna Pedestal

Axes	- azimuth and elevation
Weight	- 12,000 pounds
Azimuth coverage	- continuous 360°
Elevation coverage	- 10° to $+85^{\circ}$ (200° movement available)

Antenna System

Size	- 12 foot diameter parabola
Feed	- 4-horn monopulse
Gain	- 45 db
Beam width	- 1.1°

Transmitter

Type	- magnetron

Peak power	Frequency	Max. duty cycle
1 A.W. fixed tuned	5480 $\pm$ 35 MC	0.001
250 K.W. tunable	5450 to 5825 MC	0.0016

PRF - Internal	- 12 steps between 160 to 1707 PPS
External	- any PRF between 160 to 1707 PPS
Pulse width	- 0.25 MS, 0.5 MS and 0.1 MS
Coding	- up to 5 pulses within duty cycle limitation

Receiver System

System noise figure	- 11db
Band widths	- wide 8.0 MC - narrow 1.6 MC

Local oscillators	- two-skin and beacon
AFC	- skin and beacon

Range Tracking System

Max tracking rate	- 8,000 yds. per second
Automatic lock-on	- search ± 1000 yds. and auto lock
Servo band width	- continuously adjustable manually or automatically between 0.5 CPS (KV = 2000) and 6.0 CPS (KV = 3000)

Angle Tracking System

Max. track rate	- azimuth 40° per second elevation 30° per second
Servo band width	- continually adjustable manually or automatically between 0.5 CPS (KV = 150) and 4.0 CPS (KV = 300)

Data Outputs

Potentiometer	-
Synchro	- Army and Navy speeds
Digital	- serial straight binary range - 20 BITS (0.5 yd. quanta) angle - 17 BITS (0.05 and quanta)

Displays

Range	- dual 'A' scope dials digital - octal numeral
Angle	- dials digital - octal numeral

Cabinets

Transmitter	- 2

SCINTILLATION NOISE IN TRACKING RADARS

In 1947, an investigation was begun at the U.S. Naval research laboratory to study noise in tracking radars. Of particular interest was the noise which was found to be caused by a target when it is of finite size and complex shape; this suggested a new basis for optimum radar design. With the increasing emphasis on precision in radar guidance in the space and missile age, complete instrumentation was prepared to permit investigation of target-scintillation or target noise phenomena. While extensive theoretical studies were being carried out, the instrumentation was built to include a unique simulator, finite size targets with a complete close loop tracking system, an instrumentation radar composed of a dual channel tracking radar for measurement of components of target noise under actual tracking conditions, and equipment designed to provide automatic statistical analysis of noise data. The results of these studies showed several ways in which different components determine the choice of tracking systems and optimum design of the system. The studies revealed phenomena such as the two-reflector target, which can cause tracking errors of many target spans outside the physical extent, and a new concept of target noise in terms of a tilting of phase front of the echo signal from a target.

The noise sources which contribute to tracking noise may be separated into four components, namely servo noise, receiver noise, angle noise and amplitude noise. The first two of these

components originate in the radar itself. The second two components are called target noise, which is generated by the target when it is of finite size and complex structure. These four noise terms have been defined as follows:

1. Servo noise is the hunting action of the tracking servomechanism which results from backlash in the gears, shafts, and structures of the mount. The magnitude of this noise is essentially independent of the target and will thus be independent of range.

2. Receiver noise is the effect on the tracking accuracy of the radar of thermal noise generated in the input impedance of the receiver and any spurious hum which may be picked up by the circuitry.

3. Angle noise (angle scintillation or glint) is the tracking error introduced into the radar by variations in the apparent angle of arrival of the echo from a complex target of finite size. This effect is caused by variations in the phase front of the radiation from a multiple point target as the target changes its aspect. The magnitude of angle noise is inversely proportional to the range of the target.

4. Amplitude noise (amplitude scintillation) is the effect on the radar accuracy of fluctuations in the amplitude of the signal returned from the target. These fluctuations are caused by any change in aspect of the target and must be taken to include propeller rotation and skin vibration.

The relative amplitudes of these noise components plotted against range are as shown in Figure 21. Only two of these

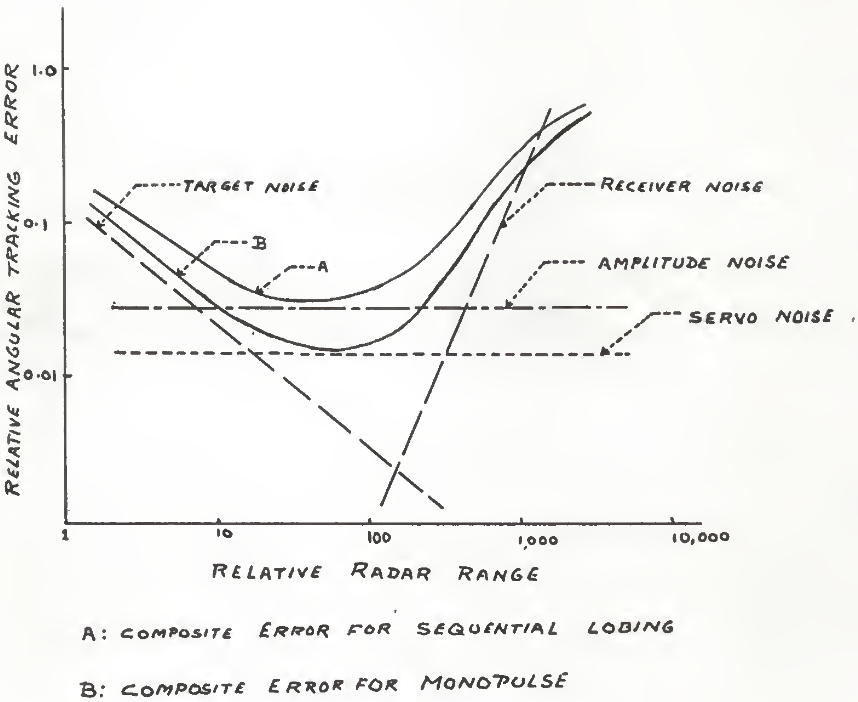


Figure 21. Relative angular tracking error caused by radar noise components as a function of range (Dunn, Howard & King, 1959).

noise factors are functions of target range. Servo noise is obviously independent of range. Receiver noise increases as the square of the range, due to the inverse fourth-power law for the echo power received. Amplitude noise, since it is interpreted by the radar as amplitude modulation of the mean signal level is independent of range if an AGC system is used. However this error does not occur in monopulse. Angle noise is a function of the linear dimension of the target and therefore varies inversely with range as long as the target subtended angle is small compared with the beam width of the antenna. Since these factors are uncorrelated the total output noise in a given tracking system adds up as shown in the Figure 21. The following is the summary of tracking error equations derived by D. K. Barton in his final report on instrumentation radar AN/FPS-16, the title of the paper being "Evaluation and Analysis of Radar Performance."

1. Thermal noise $$\sigma_t = \frac{\theta}{\sqrt{2 \frac{S}{N} \frac{f_r}{\beta_n}}} \tag{42}$$

2. Target glint $$\sigma_s \approx \frac{1}{4} \frac{L_t}{R} \tag{43}$$

3. Servo lag $$\sum = \frac{w_t}{K_v} + \frac{\dot{w}_t}{K_a} \tag{44}$$

where θ = Radar beam width

S/N = Signal to noise power ratio

f_r = Repetition rate

β_n = Servo band width

L_t = Span of target

R = Range of target

K_v = Velocity error constant

K_a = Acceleration error constant

w_t = Target angular velocity

$\dot{w}_t$ = Target angular acceleration

Another point of interest in tracking radars is their ability to resolve multiple targets. This is a complex statistical problem because of the random fluctuation of the targets, and the ability of the radar to resolve two targets can only be expressed as a probability. The Figures 22-a, 22-b, 22-c show the probability distribution of the tracking point of a radar looking at two targets separated by different fractions of the antenna beam width (A. J. Stecca and N. V. O'Neal, 1956). From those three Figures it is seen that the resolution is at its best when the target separation increases beyond 0.85 times the antenna beam width.

A special condition of target noise as discussed earlier, is the simple target composed of two reflectors. This simplified target is particularly significant because it is a close approximation of the low angle tracking problem. This problem occurs when the radar sees the target plus its image reflected from the surface and serious resultant elevation tracking errors render the elevation data almost useless.

Two reflector phenomena are analyzed (Meade, 1950) and it is shown that the point tracked by the radar is the function

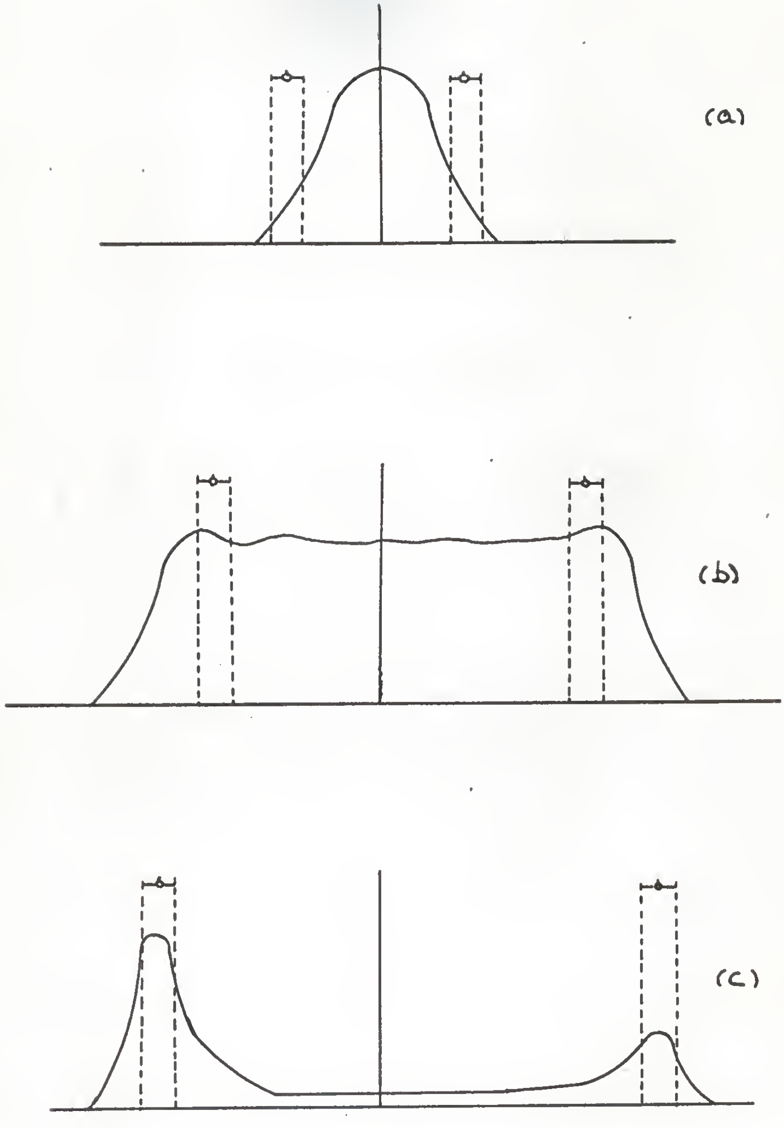


Figure 22. Probability distributions of radar-pointing angle when tracking two targets for three different angular separations of the targets (a) 0.30 antenna beam width (b) 0.75 antenna beam width (c) 0.85 antenna beam width (Stecca & O'Neal, 1956).

shown below.

$$E = \left(\frac{1}{2}\right) \left(\frac{1 - a^2}{1 + a^2 + 2a \cos (\phi_1 - \phi_2)}\right) \tag{45}$$

Where L = is the target reflector spacing in either linear or angular units.

$\phi_1 - \phi_2$ = is the reflective phase of the echoes from the two target reflectors.

a = is the amplitude ratio of the echoes from the two reflectors.

This function is plotted in Figure 23. The plot of Figure 23 shows the apparent location of the target as seen by the radar. It can be seen that the maximum error occurs at 180-degree relative phase where the echo amplitude is at a minimum because the echoes from the two reflectors subtract. Therefore there is a negative correlation between echo amplitude and the magnitude of the error.

In concluding the discussion on scintillation noise the following points are to be noted.

1. Amplitude noise causes noise independent of target range in lobing or scanning radars because of the high frequency components which fall in the vicinity of the lobing or scanning rates. The effect is eliminated by the proper use of monopulse-tracking techniques.

2. Angle noise is a function of target size and shape; therefore its magnitude varies inversely with range.

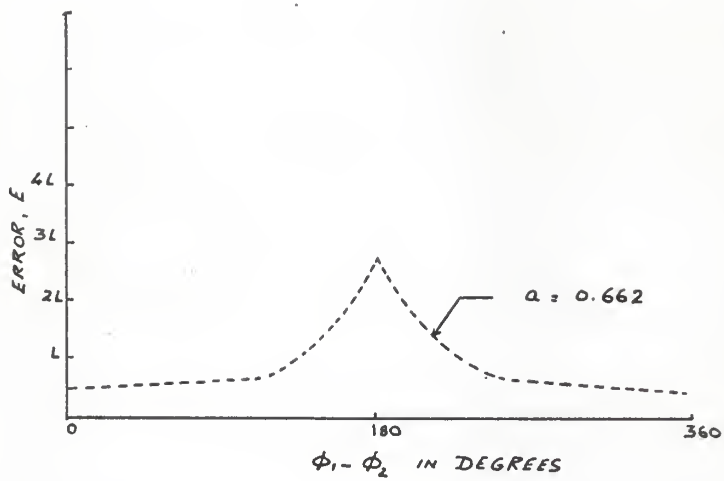


Figure 23. Apparent location of the two reflector target as a function of relative phase (Meade, 1955).

3. Servo band width should be kept to the minimum consistent with tactical requirements to minimize target noise effects.

4. The two reflector target phenomenon shows that the angle noise can cause the target to appear many target spans outside the physical extent of the target. This phenomenon also demonstrates how the low angle target causes severe tracking errors.

5. It is demonstrated that a radar can resolve multiple targets when the target separation is in the vicinity of 0.8 times the antenna beam width or greater.

MONOPULSE SYSTEM PARAMETERS

The basic difference between a phase-sensing and amplitude-sensing monopulse system lies in the antenna configuration; and therefore major attention is given to the antenna and the microwave assembly which produces the monopulse additions and subtractions. Physically the comparator and the receiving equipment can be the same for both the systems, but the exact function the comparator performs and the errors introduced by its use are quite different for each sensing system.

Amplitude-sensing monopulse system: Antenna parameters. From the Figure 24 we see that

ψ = Beam separation

ϵ = Beam width

θ_{NA} = Angle at which the first null of lobe A occurs in the domain

$$0^\circ < \theta < -90^\circ$$

θ_{NB} = Angle at which the first null of lobe B occurs in the domain

$$0^\circ < \theta < -90^\circ$$

θ = Angle of the return signal wavefront with respect to the plane of the antenna aperture.

It is assumed that the antenna voltage radiation pattern, produced by the displaced phase centers of the feed horns are described for lobe A by

$$\sin \frac{\pi(\theta - \theta_{NA})}{\epsilon} \qquad \theta_{NA} \leqslant \theta < \theta_{NA} + \epsilon \tag{46}$$

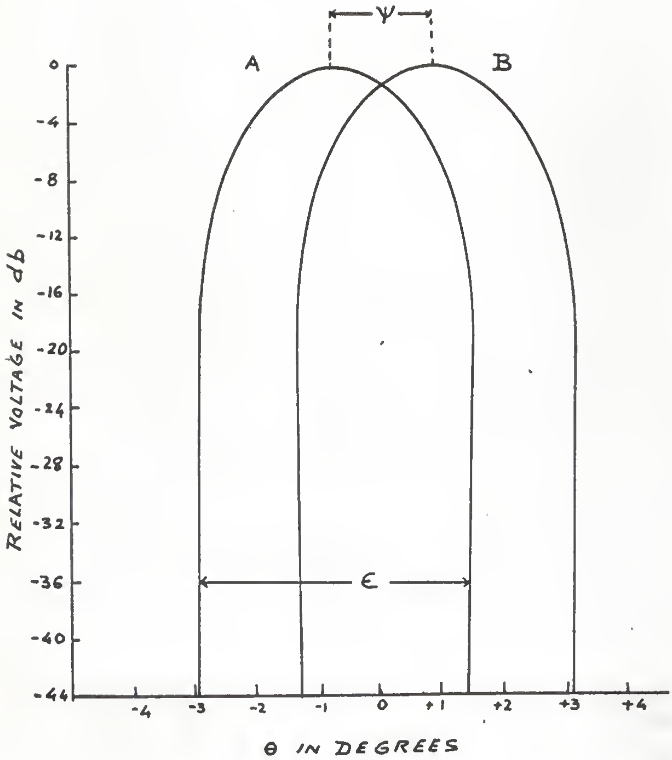


Figure 24. Antenna lobes of an amplitude-sensing system assuming sine radiation pattern.

and for lobe B by

$$\sin \frac{\pi(\theta - \theta_{NB})}{\epsilon} \qquad \theta_{NB} \leqslant \theta \leqslant \theta_{NB} + \epsilon \tag{47}$$

A sine function was chosen to describe the amplitude radiation patterns instead of the more common $\frac{\sin X}{X}$ expression, since a good approximation of the actual patterns is obtained and it simplifies the expressions that will be derived.

The separation between the two lobes A and B can be defined as $\psi = \theta_{NB} - \theta_{NA}$.

If the value of ψ is small, it can be computed approximately from the antenna parameters by the following expression (Fry & Coward, 1950).

$$\psi = \theta_{NB} - \theta_{NA} = Kp \operatorname{Tan}^{-1} \frac{n}{f} \tag{48}$$

Where n is the distance between the feed horn centers and f is the focal length of the dish in the desired plane. Kp is a constant which is a function of the size and shape of the paraboloid and the type of illumination used across the aperture. Kp = 0.6 for a small dish.

The equations for the two lobes can be rewritten in a form which shows explicitly the antenna parameters of beam width ϵ and beam separation ψ. It can be seen from the diagram of lobe patterns

$$\theta_{NA} = -\tfrac{1}{2} (\epsilon + \psi)$$

and $\theta_{NB} = -\tfrac{1}{2} (\epsilon - \psi)$

Then the expression for lobe A becomes

$$\sin\left[\frac{\pi\theta}{\epsilon} + \frac{\pi}{2}\left(1 + \frac{\psi}{\epsilon}\right)\right] \qquad (49)$$

$$-\tfrac{1}{2}(\epsilon + \psi) \leqslant \theta \leqslant \tfrac{1}{2}(\epsilon - \psi)$$

and for lobe B

$$\sin\left[\frac{\pi\theta}{\epsilon} + \frac{\pi}{2}\left(1 - \frac{\psi}{\epsilon}\right)\right]$$

$$-\tfrac{1}{2}(\epsilon - \psi) \leqslant \theta \leqslant \tfrac{1}{2}(\epsilon + \psi) \qquad (50)$$

Phase shift effects. It has been assumed that an equal phase signal is being received by both horns near the position of the null (i.e: $\theta = 0$). However, as a result of some phase shift, γ, in the reflector, feed horn and comparator (which will be termed pre-comparator phase shifts) the voltages from the two lobes will not cancel at the boresight and the null level of the difference pattern will not be zero.

For signals arriving on the boresight axis ($\theta = 0$) the magnitude of lobe A equals the magnitude of lobe B.

$$\sin\frac{\pi}{2}\left(1 + \frac{\psi}{\epsilon}\right) = \sin\frac{\pi}{2}\left(1 - \frac{\psi}{\epsilon}\right) = \cos\frac{\pi}{2}\frac{\psi}{\epsilon} \qquad (51)$$

However if there is a pre-comparator phase shift, γ, these signals are not 180° out-of-phase, and will produce a resultant output where magnitude is (Cohen & Steinmetz, 1959)

$$\sin\frac{\pi}{2}\left(1 + \frac{\psi}{\epsilon}\right)\sqrt{2(1 - \cos\gamma)}$$

$$= 2\cos\left(\frac{\pi}{2}\frac{\psi}{\epsilon}\right)\sin\tfrac{1}{2}\gamma \qquad (52)$$

The null depth is defined as the ratio of the level in the null to the level at the peak of the difference pattern. The peak occurs at

$$\frac{d}{d\theta} \sin \left[\frac{\pi\theta}{\epsilon} + \frac{\pi}{2} \left(1 + \frac{\psi}{\epsilon}\right) \right] = 0 \tag{53}$$

$$\frac{\epsilon}{2} \leqslant \psi \leqslant \epsilon$$

from which $\theta = -\psi/2$. Substituting back into the lobe equation a value of one is obtained which is the peak of the difference pattern when $\frac{\epsilon}{2} \leqslant \psi < \epsilon$. Therefore the null depth in db for large beam separation is

$$20 \log_{10} \left(\frac{1}{2 \cos \left(\frac{\pi \psi}{2\epsilon}\right) \sin \frac{1}{2}\gamma} \right) \tag{54}$$

However when the beam separation is less than $\epsilon/2$ the null depth ratio changes because the peak amplitude is no longer one. It can be seen that the peak amplitude will always occur at θ_{NB} for smaller beam separation. Hence the null depth in db for domain $0 < \psi < \epsilon/2$ is

$$20 \log_{10} \left(\frac{\sin \frac{\pi}{2} \frac{\psi}{\epsilon}}{\sin \frac{1}{2}\gamma} \right) \tag{55}$$

A family of curves showing the effects of phase shift, γ, on null depth as a function of ratio of beam separation and beam width is given in Figure 25. Since the null depth will affect the resolution of the radar system and its angle measurement precision, it is most desirable to keep the null depth as deep

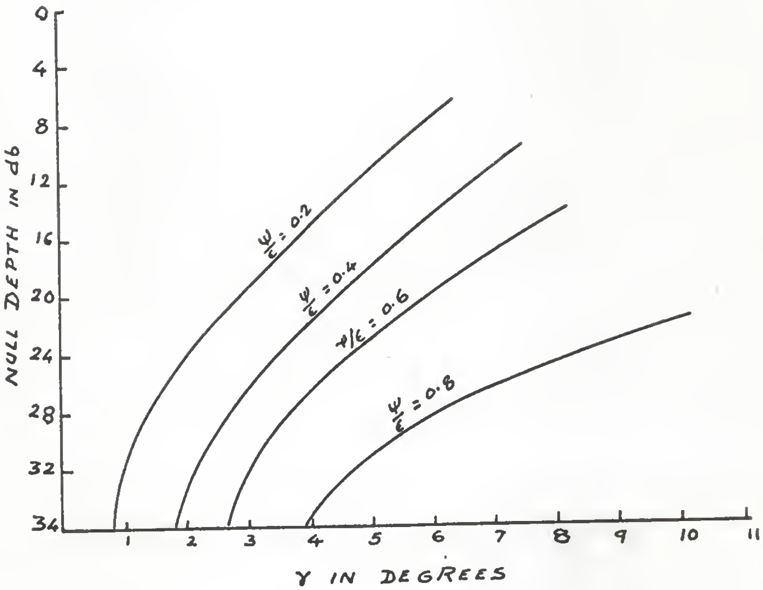


Figure 25. Null depth vs. pre-comparator phase shift for an amplitude-sensing monopulse system (Cohen & Steinmetz, 1959).

and sharp as possible. The Figure 25 indicates that for good null depths pre-comparator phase shifts must be kept small and for a given amount of phase shift in the feed, better null depths are obtained for the largest possible $\frac{\psi}{\epsilon}$ ratio. Using narrow beam widths and increasing beam separation will cause the sum pattern to flatten until eventually an undesirable dip occurs in the pattern. Other factors such as the allowable phase center separation of the feed horns and dish size will also influence the engineering compromise required to obtain optimum system performance.

Pre-comparator phase shifts, in addition to increasing the null depth also shifts the phase crossover; or in other words the antenna boresight indication.

We have found out the magnitude of difference channel in Equation 52. Its phase angle is found to be (W. Cohen & C. M. Steinmetz, 1959)

$$\alpha_D = \mathrm{Tan}^{-1} \frac{\sin \gamma \sin \left[\frac{\pi\theta}{\epsilon} + \frac{\pi}{2}\left(1 + \frac{\psi}{\epsilon}\right)\right]}{\sin\left[\frac{\pi\theta}{\epsilon} + \frac{\pi}{2}\left(1 - \frac{\psi}{\epsilon}\right)\right] - \sin\left[\frac{\pi\theta}{\epsilon} + \frac{\pi}{2}\left(1 + \frac{\psi}{\epsilon}\right)\right] \cos \gamma} \tag{56}$$

Similarly for the sum channel the phase angle is found to be

$$\alpha_S = \mathrm{Tan}^{-1} \frac{-\sin \gamma \sin \left[\frac{\pi\theta}{\epsilon} + \frac{\pi}{2}\left(1 + \frac{\psi}{\epsilon}\right)\right]}{\sin\left[\frac{\pi\theta}{\epsilon} + \frac{\pi}{2}\left(1 - \frac{\psi}{\epsilon}\right)\right] + \sin\left[\frac{\pi\theta}{\epsilon} + \frac{\pi}{2}\left(1 + \frac{\psi}{\epsilon}\right)\right] \cos \gamma} \tag{57}$$

The phases of these two signals are compared in the receiver's amplitude-sensitive phase detector. The phase reversal point of the detector's output voltage is an indication of the antenna boresight. Any shift in this phase reversal point corresponds to an error in the pointing accuracy of the antenna. Then the difference between the two phase angles determines the response of the detector.

The plots of Figures 26a, 26b show $(\alpha_S - \alpha_D)$, the phase comparison of the difference and sum channel resultant signal for selected values of γ and ϵ, with varying ψ/ϵ ratio; and, selected values of ϵ and ψ/ϵ with varying γ. It can be seen from the plots of Figure 26a and 26b that the phase of the compared signals reverses sharply when there is no pre-comparator phase shift, and becomes more gradual with increasing amounts of pre-comparator phase shifts or smaller $\frac{\psi}{\epsilon}$ ratio.

It should be noted that in all cases with no post-comparator phase shift the reversal occurs on the boresight. However the post-comparator phase shifts change the point at which the curve intersects the detector phase reversal point. Hence the combination of pre-comparator and post comparator phase shifts will result in a change of boresight indication.

Voltage unbalance effects. As previously stated, the null point should occur at the antenna boresight ($\theta = 0^{\circ}$) for symmetrical antenna patterns, when both lobes are of equal magnitude

$$\text{i.e.:} \quad \sin \frac{\pi}{2} \left(1 + \frac{\psi}{\epsilon}\right) = \sin \frac{\pi}{2} \left(1 - \frac{\psi}{\epsilon}\right) \qquad (58)$$

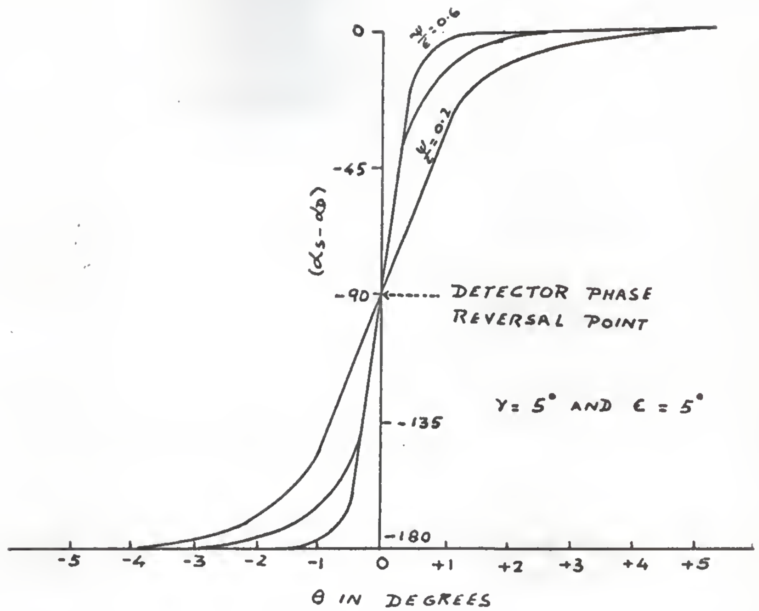


Figure 26-a. Phase difference $(\alpha_S - \alpha_D)$ vs. angle θ for various ratios of ψ/ϵ for amplitude-sensing monopulse (Cohen & Steinmetz, 1959).

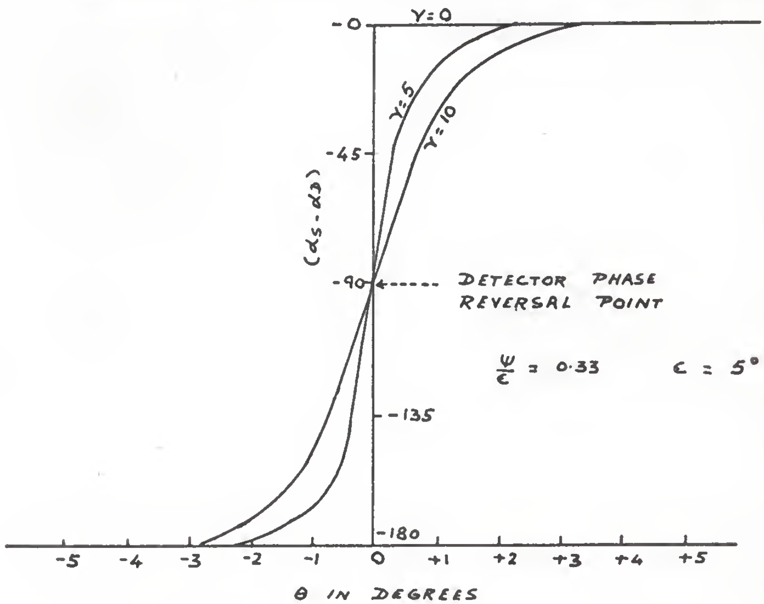


Figure 26-b. Phase difference $(\alpha_S - \alpha_D)$ vs. angle θ for various pre-comparator phase shift (Cohen & Steinmetz, 1959).

This equality holds true when there is a perfect voltage balance between the two channels A and B. Should the signal levels be unequal, due to more attenuation in one channel than the other, the Equation 58 can be re-written as

$$\sin\left[\frac{\pi\theta}{\epsilon} + \frac{\pi}{2}\left(1 + \frac{\psi}{\epsilon}\right)\right] = K \sin\left[\frac{\pi\theta}{\epsilon} + \frac{\pi}{2}\left(1 - \frac{\psi}{\epsilon}\right)\right] \qquad (59)$$

where $K < 1$ represents the loss in relative voltage of the weaker signal channel. In order to solve this equation for θ_S which will now indicate the boresight shift, let $A = \frac{\pi\theta_S}{\epsilon}$, $B = \frac{\pi}{2}\left(1 + \frac{\psi}{\epsilon}\right)$ and $C = \frac{\pi}{2}\left(1 - \frac{\psi}{\epsilon}\right)$.

Thus the above equation can be written as $\sin(A + B) = K \sin(A + C)$.

By grouping terms

$$A = \tan^{-1} \frac{K \sin C - \sin B}{\cos B - K \cos C} \qquad (60)$$

Therefore the boresight shift as a function of voltage unbalance is

$$\theta_S = \frac{\epsilon}{\pi} \tan^{-1} \frac{K \sin\left[\frac{\pi}{2}\left(1 - \frac{\psi}{\epsilon}\right)\right] - \sin\left[\frac{\pi}{2}\left(1 + \frac{\psi}{\epsilon}\right)\right]}{\cos\left[\frac{\pi}{2}\left(1 + \frac{\psi}{\epsilon}\right)\right] - K \cos\left[\frac{\pi}{2}\left(1 - \frac{\psi}{\epsilon}\right)\right]}$$

$$= \frac{\epsilon}{\pi} \tan^{-1} \frac{1 - K}{1 + K} \cot \frac{\pi}{2} \frac{\psi}{\epsilon} \qquad (61)$$

The above equation divided by ϵ is plotted as a function of various $\frac{\psi}{\epsilon}$ ratios in Figure 27. Multiplying the factor obtained from the curve, by ϵ, one arrives at the boresight shift in

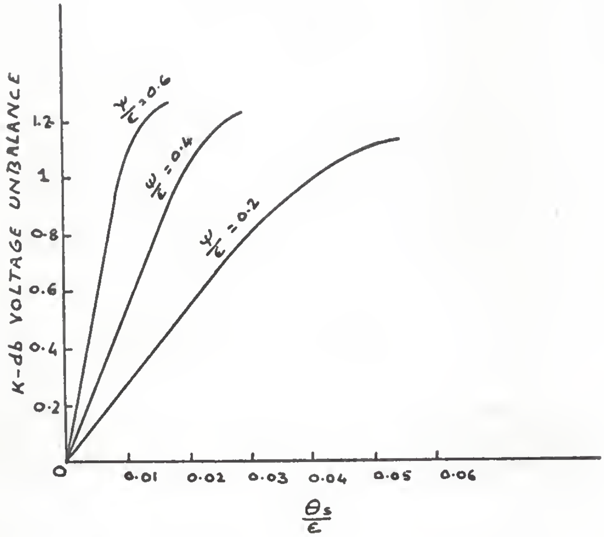


Figure 27. Boresight shift vs. pre-comparator voltage unbalance for amplitude-sensing monopulse system (Cohen & Steinmetz, 1959).

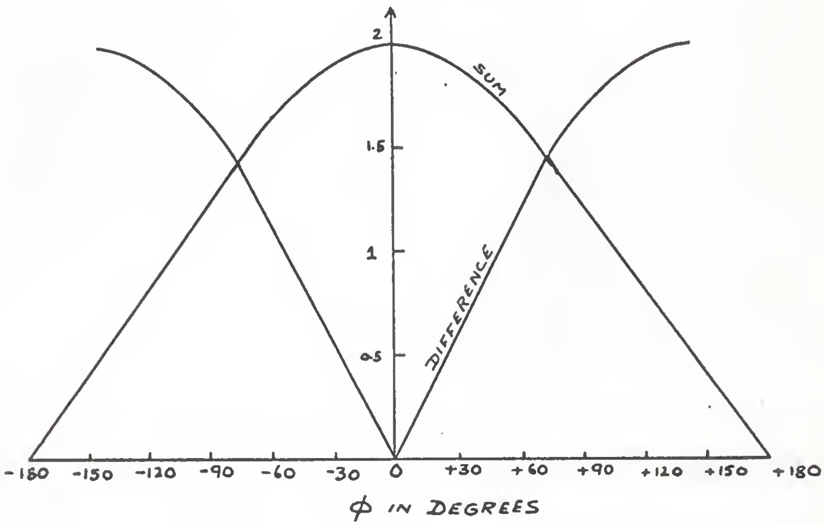


Figure 28. Signal amplitude of sum and difference channels in a phase sensing monopulse system.

degrees. It can be seen that the greater the value of the ratio $\frac{\psi}{\epsilon}$, the smaller will be the boresight shift for a given voltage unbalance.

Phase-sensing monopulse system. In a phase sensing monopulse system we know that the phase delay ϕ due to the separation 'd' of the two antennas is equal to $\frac{2\pi d \sin\theta}{\lambda}$

$$\phi = \frac{2\pi d \sin\theta}{\lambda} \qquad (62)$$

where θ = angle at which the radar energy returns. The antenna voltages may be given as follows

$$A = K_1 \sin(w_c t + \phi) \qquad (63)$$

$$B = K_1 \sin w_c t \qquad (64)$$

where w_c is the angular velocity of the carrier and K_1 an arbitrary value which is related to the transmitted power, range, backscattering conditions and antenna parameters.

For the difference channel (A - B) we have

$$E_D = K_1 \left[\sin(w_c t + \phi) - \sin w_c t \right] \qquad (65)$$

The resultant output E_D, is then composed of the subtraction of two voltages of the same frequency but of changing phase. This expression can be re-written as a single resultant voltage and phase angle as follows

$$E_D = K_D \sin(w_c t + \alpha_D) \qquad (66)$$

where $K_D = K_1 \sqrt{(\cos \phi - 1)^2 + (\sin \phi)^2} = 2 K_1 \sin \tfrac{1}{2}\phi$ (67)

and

$$\alpha_D = \mathrm{Tan}^{-1} \left[\frac{\sin \phi}{\cos \phi - 1} \right] \quad (68)$$

The phase angle expression can be simplified further and may be expressed in two ways

$$\alpha_D = \frac{\pi}{2} + \tfrac{1}{2}\phi \qquad 0^\circ < \phi < 360^\circ \quad (69)$$

or $$\alpha_D = \frac{\pi}{2} + \tfrac{1}{2}\phi \qquad 0^\circ < \phi < +180^\circ \quad (70)$$

$$\alpha_D = \frac{3\pi}{2} + \tfrac{1}{2}\phi \qquad 0^\circ > \phi > -180^\circ \quad (71)$$

Similarly for the sum channel we have

$$E_S = K_1 \left[\sin w_c t + \sin (w_c t + \phi) \right] \quad (72)$$

or $$E_S = K_S \sin (w_c t + \alpha_s)$$

where $K_S = K_1 \sqrt{(1 + \cos \phi)^2 + (\sin \phi)^2}$

$$= 2K_1 \cos \tfrac{1}{2}\phi \quad (73)$$

and $$\alpha_S = \mathrm{Tan}^{-1} \left(\frac{\sin \phi}{1 + \cos \phi} \right) \quad (74)$$

The sum channel phase expression can also be simplified and may be expressed as

$$\alpha_S = \tfrac{1}{2}\phi \qquad 180^\circ > \phi > -180^\circ \quad (75)$$

Using the above derived equations, the relative amplitude of the sum and difference channels as a function of $\emptyset$ are plotted as shown in Figure 28. Comparison of the phase angles of the sum and difference signals yield the following result

$$\alpha_S - \alpha_D = \frac{1}{2}\emptyset - \frac{\pi}{2} + \frac{1}{2}\emptyset = -\frac{\pi}{2} \qquad 0^\circ < \emptyset < +180^\circ \qquad (76)$$

$$\alpha_S - \alpha_D = \frac{1}{2}\emptyset - \frac{3\pi}{2} + \frac{1}{2}\emptyset = -\frac{3\pi}{2} \qquad 0^\circ > \emptyset > -180^\circ \qquad (77)$$

Phase shift effects. If it is assumed that a phase delay γ, occurs in the antenna feed, B, the corresponding equations change as follows

$$E_{S_1} = K_{S_1} \sin\left[w_c t + \mathrm{Tan}^{-1} \frac{\sin\emptyset - \sin\gamma}{\cos\emptyset + \cos\gamma}\right] \qquad (78)$$

$$\alpha_{S_1} = \mathrm{Tan}^{-1}\left[\frac{\sin\emptyset - \sin\gamma}{\cos\emptyset + \cos\gamma}\right] \qquad (79)$$

$$\text{or } \alpha_{S_1} = \tfrac{1}{2}(\emptyset - \gamma) \qquad 180^\circ > \emptyset + \gamma > -180^\circ \qquad (80)$$

Similarly for the difference channel

$$\alpha_{D_1} = \mathrm{Tan}^{-1} \frac{\sin\emptyset + \sin\gamma}{\cos\emptyset - \cos\gamma} \qquad (81)$$

$$\text{or } \alpha_{D_1} = \frac{\pi}{2} - \frac{1}{2}(\gamma - \emptyset) \qquad 0^\circ < \gamma + \emptyset < +180^\circ \qquad (82)$$

$$\alpha_{D_1} = \frac{3\pi}{2} - \frac{1}{2}(\gamma - \emptyset) \qquad 0^\circ > \gamma + \emptyset > -180^\circ \qquad (83)$$

The phase difference between the sum and difference channels

$\alpha_{S_1} - \alpha_{D_1}$ will equal the following expressions

$$\alpha_{S_1} - \alpha_{D_1} = -\frac{\pi}{2} \quad 0^\circ < \gamma + \phi < +180^\circ \tag{84}$$

$$\alpha_{S_1} - \alpha_{D_1} = -\frac{3\pi}{2} \quad 0^\circ > \gamma + \phi > -180^\circ \tag{85}$$

The two conditions, before and after the null, are similar to those calculated before, except that the phase reversal occurs when $\phi = -\gamma$ and not when $\phi = 0$. A plot of $(\alpha_S - \alpha_D)$ with and without the error γ is shown in Figure 29. It can be seen from the Figure 29 that as to how the phase reversal point advances because of a pre-comparator phase shift of $\gamma = +10^\circ$.

Similarly it can be shown that the amplitude null advances the same amount as the phase reversal point advances for the same phase delay γ (W. Cohen & C. M. Steinmetz, 1959).

Thus it may be seen that the amount of null or phase reversal shift for a given phase shift depends on the value $\frac{2\pi d}{\lambda}$.

The effect of the $\frac{d}{\lambda}$ ratio on the amount the null and phase reversal shift is shown in Figure 30. It is observed that greater the value of $\frac{d}{\lambda}$ the less will be the shift. This demonstrates that in designing a phase-sensing system the spacing of the antennas and the wave length of the carrier are important parameters in determining the errors that will be encountered in the operation of the system.

Voltage unbalance effects. Let the voltage in A channel be reduced by a factor $L < 1$. The corresponding equations

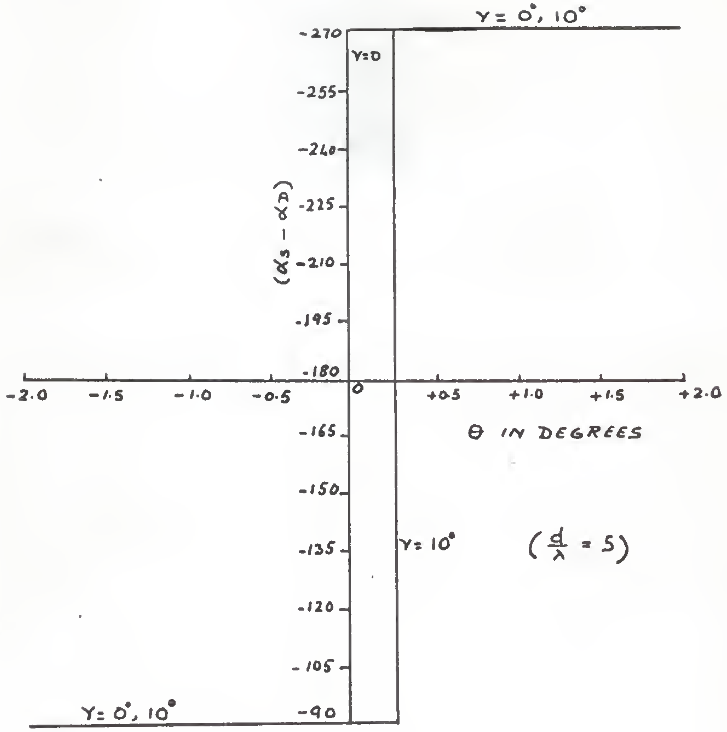


Figure 29. Phase difference vs. angle in a phase-sensing system (Cohen & Steinmetz, 1959).

change as follows.

For the difference channel

$$E_{D_2} = K_{D_2}\left[\sin w_c t + \mathrm{Tan}^{-1}\left(\frac{\sin \phi}{\cos \phi - L}\right)\right] \tag{86}$$

where $K_{D_2} = K_1 \sqrt{(\cos \phi - L)^2 + (\sin \phi)^2}$ (87)

and $\alpha_{D_2} = \mathrm{Tan}^{-1}\left(\frac{\sin \phi}{\cos \phi - L}\right)$ (88)

Similarly for the sum channel voltage under these conditions we find

$$E_{S_2} = K_{S_2}\left[\sin w_c t + \mathrm{Tan}^{-1}\left(\frac{\sin \phi}{L + \cos \phi}\right)\right] \tag{89}$$

where $K_{S_2} = K_1 \sqrt{(L + \cos \phi)^2 + (\sin \phi)^2}$ (90)

A plot of these equations for amplitude effects is as shown in Figure 31. The sum channel amplitude does not change but it is apparent from the above plot as to how the difference null fills in. When these null fills in the resolution of the radar system declines.

It is also shown (Cohen & Steinmetz, 1959) that the sharp phase transition at $\phi = 0$ becomes more gradual as the voltage unbalance is increased. This is similar to amplitude sensing system. Here also the post-comparator phase shifts will cause a reversal in phase at a point other than $\phi = 0$ which would indicate an error in the boresight. This results in the same effect as for amplitude sensing system.

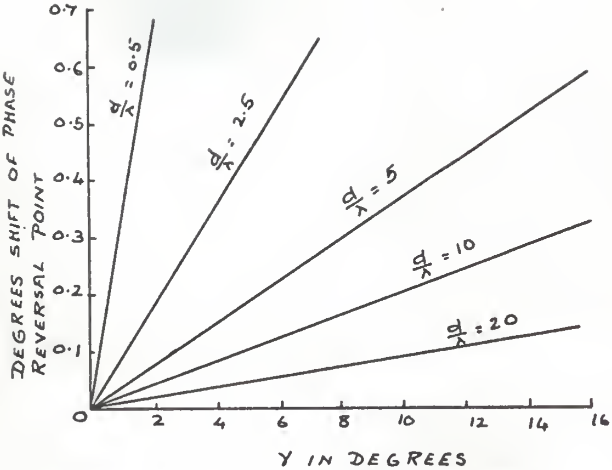


Figure 30. Null or phase reversal shift vs. pre-comparator phase shift in a phase sensing monopulse system (Cohen & Steinmetz, 1959).

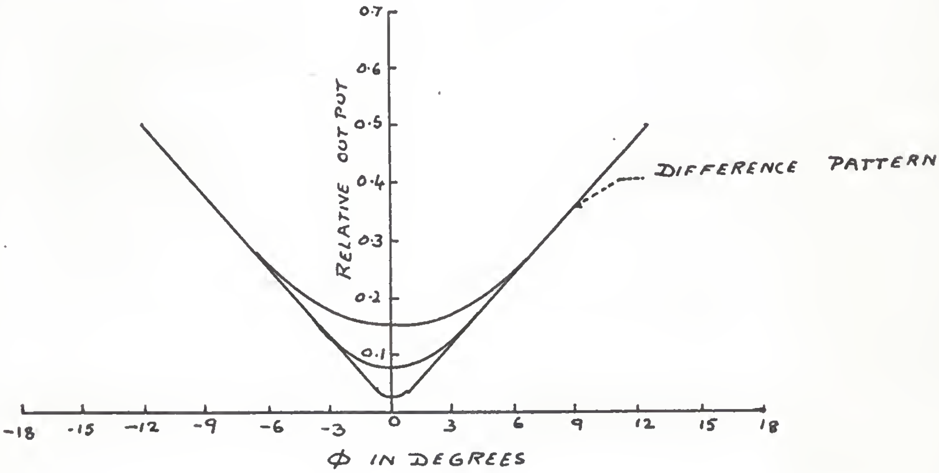


Figure 31. Amplitude of sum and difference channels with voltage unbalance in a phase-sensing monopulse system (Cohen & Steinmetz, 1959).

CONCLUSIONS

Among the four continuous tracking radars (sequentially lobed, conical scan, amplitude and phase comparison), conical scan and amplitude comparison radars are most frequently used. The phase comparison monopulse radar is not in much use because of the disadvantage that one has to incorporate two antennas in it and the accompanying loss in its effective aperture. Conical scan is preferred over sequentially lobed radar because of ease in operation. The conical scan system is compared below with amplitude comparison monopulse radar in regards to detectability, tracking accuracy and complexity.

As far as the detectability is concerned, there is no significant difference between conical scan and amplitude comparison radar, when the major parameters of the radar considered in the radar equation are the same in both cases. However both of these systems suffer a slight loss of antenna gain in comparison with non-tracking radars of the same size because of the offset antenna beams.

Amplitude comparison radar has a better tracking accuracy then the conical scan because of degradation introduction by the amplitude fluctuations, which do not occur in the monopulse systems. However for equal signal to noise ratios and antenna beam widths the tracking accuracy of the two systems are comparable in the absence of amplitude fluctuations.

Monopulse radars are generally more complex than the conical scan radars. Three separate receivers are necessary

to obtain the error signal in two orthogonal coordinates. The conical scan radars require only one receiver. In the amplitude comparison monopulse radar system, the gain and the phase shift in the three channels must be kept identical lest it might introduce error components.

Since with monopulse tracking radar it is possible in principle to obtain the angular error on the basis of a single pulse, it is thus theoretically possible to obtain the angle information in microseconds in comparison with milliseconds in conical scan.

ACKNOWLEDGMENT

The author wishes to express his deep appreciation of the guidance given by his major adviser, Dr. H. S. Hayre.

BIBLIOGRAPHY

1. Skolnik, Merril I.
   Introduction to radar systems. McGraw-Hill Book Company, Inc., 1962.

2. Rhodes, D. R.
   Introduction to monopulse. McGraw-Hill Book Company, Inc., 1959.

3. Page, R. N.
   Monopulse radar, IRE convention record, part 1, pp. 132-136, 1955.

4. Dunn, J. H. and Howard, D. D.
   Precision tracking with monopulse radar. Electronics, Vol. 33, No. 17, pp. 51-56, April 22, 1960.

5. Barton, D. K. and Sherman, S. M.
   Pulse radar for trajectory instrumentation, paper presented at sixth national flight test instrumentation symposium, Instrument Society of America, San Diego, California, May 3, 1960.

6. Cohen, W. and Steinmetz, C. M.
   Amplitude and phase sensing monopulse system parameters. Pts I and II, Microwave J., Vol. 2, pp. 27-33, October, 1959, and pp. 33-38, November, 1959.

7. Dunn, J. H., Howard, D. D. and King, A. M.
   Phenomena of scintillation noise in radar tracking systems, proc. IRE, Vol. 47, pp. 855-863, May, 1959.

8. Barton, D. K.
   Accuracy of a monopulse radar, proc. third national convention on mil. electronics by PGME of IRE, 1959.

9. Stecca, A. J. and O'Neal, N. V.
   Target noise simulator closed loop tracking. U.S. Naval Research Lab., Washington, D.C., Rep. No. 4770, July, 1956.

10. Meade, J. E.
   Target considerations in A. S. locke. Guidance, D. Van Nostrand Co., Inc., Princeton, New Jersey, Ch. 11, pp. 440-442, 1955.

A STUDY OF MONOPULSE TRACKING
RADAR SYSTEMS

by

SULTAN M. ZIA

B.E., B.M.S. College of Engineering
University of Mysore, India, 1962

AN ABSTRACT OF A MASTER'S REPORT

submitted in partial fulfillment of the

requirements of the degree

MASTER OF SCIENCE

Department of Electrical Engineering

KANSAS STATE UNIVERSITY
Manhattan, Kansas

1965

ABSTRACT

The techniques for extracting angle as well as range information for tracking a target from the return of a single radar pulse are discussed. The essential characteristics of the various forms of monopulse are deduced and developed into a unified theory from a set of three basic postulates. These postulates are the explicit statements of the physical characteristics common to all monopulse systems. It is shown that there are three and only three distinct classes of angle detection possible and hence only three distinct classes of monopulse possible. The three classes are pure amplitude, pure phase and sum-and-difference. Monopulse systems of the three distinct classes are described in detail first in two dimension and later dual plane monopulse systems are also included.

Scintillation noise in tracking radars is studied and it is concluded that by the introduction of monopulse systems the amplitude noise is completely eliminated. The study also revealed the phenomena such as the two reflector target which can cause tracking errors of many target spans outside the physical extent of the target.

Finally an analysis of amplitude and phase sensing, sum and difference monopulse systems is made in an attempt to specify the effect certain parameters have on system performance. Equations describing the performance of the systems are derived and the system evaluation curves are also included.